Wetlands (2024) 44:1
https://doi.org/10.1007/s13157-023-01751-x

ORIGINAL RESEARCH ARTICLE

On the Relationship Between Aquatic CO_2 Concentration and Ecosystem Fluxes in Some of the World's Key Wetland Types

Jessica L. Richardson[1] · Ankur R. Desai[2] · Jonathan Thom[3] · Kim Lindgren[4] · Hjalmar Laudon[5] · Matthias Peichl[5] · Mats Nilsson[5] · Audrey Campeau[5] · Järvi Järveoja[5] · Peter Hawman[6] · Deepak R. Mishra[6] · Dontrece Smith[7] · Brenda D'Acunha[8] · Sara H. Knox[9] · Darian Ng[9] · Mark S. Johnson[8] · Joshua Blackstock[10] · Sparkle L. Malone[11] · Steve F. Oberbauer[12] · Matteo Detto[13] · Kimberly P. Wickland[14] · Inke Forbrich[15] · Nathaniel Weston[16] · Jacqueline K. Y. Hung[17] · Colin Edgar[18] · Eugenie S. Euskirchen[18] · Syndonia Bret-Harte[18] · Jason Dobkowski[19] · George Kling[19] · Evan S. Kane[20] · Pascal Badiou[21] · Matthew Bogard[22] · Gil Bohrer[23] · Thomas O'Halloran[24] · Jonny Ritson[25] · Ariane Arias-Ortiz[26] · Dennis Baldocchi[26] · Patty Oikawa[27] · Julie Shahan[28] · Maiyah Matsumura[22]

Received: 13 July 2023 / Accepted: 1 November 2023

Abstract

To understand patterns in CO_2 partial pressure (P_{CO2}) over time in wetlands' surface water and porewater, we examined the relationship between P_{CO2} and land–atmosphere flux of CO_2 at the ecosystem scale at 22 Northern Hemisphere wetland sites synthesized through an open call. Sites spanned 6 major wetland types (tidal, alpine, fen, bog, marsh, and prairie pothole/karst), 7 Köppen climates, and 16 different years. Ecosystem respiration (R_{eco}) and gross primary production (GPP), components of vertical CO_2 flux, were compared to P_{CO2}, a component of lateral CO_2 flux, to determine if photosynthetic rates and soil respiration consistently influence wetland surface and porewater CO_2 concentrations across wetlands. Similar to drivers of primary productivity at the ecosystem scale, P_{CO2} was strongly positively correlated with air temperature (T_{air}) at most sites. Monthly average P_{CO2} tended to peak towards the middle of the year and was more strongly related to R_{eco} than GPP. Our results suggest R_{eco} may be related to biologically driven P_{CO2} in wetlands, but the relationship is site-specific and could be an artifact of differently timed seasonal cycles or other factors. Higher levels of discharge do not consistently alter the relationship between R_{eco} and temperature normalized P_{CO2}. This work synthesizes relevant data and identifies key knowledge gaps in drivers of wetland respiration.

Keywords Wetlands · Carbon Dioxide · Dissolved CO2 · Biogeochemistry · Emissions · Flux

Introduction

Refining our Understanding of the Wetland C Cycle

Global wetlands may contain as much as 71% of the biological carbon (C) stored on land, despite making up less than 9% of global land area (Mitra et al. 2005; Zedler & Kercher 2005). To understand the potential for wetlands to maintain C pools under changing conditions, we must evaluate how C moves into and out of wetland ecosystems. Lateral C export from wetlands is a crucial part of understanding global wetland C storage capacity. Comparing wetland dissolved CO_2 concentrations to net ecosystem exchange (NEE, the net CO_2 flux from ecosystem to atmosphere) could improve our understanding of the relationship between vertical C fluxes (NEE, gross primary productivity (GPP), and ecosystem respiration (R_{eco})) and lateral loss or movement of C (dissolved organic carbon (DOC), dissolved inorganic carbon (DIC)) (Bogard et al. 2020). NEE is unlike net ecosystem production (NEP) in that it represents *observed* land–atmosphere gas exchange and captures CO_2 fluxes from fire but does not reflect upwelling or lateral or vertical mixing of aquatic DIC (Chapin et al. 2006).

While vertical fluxes explain the exchange of C between ecosystems and the atmosphere, lateral fluxes indicate horizontal transport away from the ecosystem where C was initially fixed by photosynthesis (Ciais et al. 2008). Lateral fluxes depend on landscape connectivity, the concentration of C in surface water, and water flow (whether from groundwater, surface water, or precipitation). CO_2 partial pressure

Extended author information available on the last page of the article

Published online: 05 December 2023

(P_{CO2}) is a component of DIC related to the concentration of dissolved CO_2 in water and is an important aspect of measuring lateral gas exchange, especially at low pH (Megonigal & Neubauer 2009). We ask three main questions about lateral and vertical CO_2 flux through this work:

1. What are the average wetland water (soil porewater and surface water) P_{CO2} concentrations?
2. Through which processes are lateral and vertical C flux components linked?
3. How does discharge mediate the relationship between P_{CO2} and vertical fluxes, if at all?

We hypothesize that GPP and R_{eco} contribute to the biologically derived component of P_{CO2} in wetlands when there is low lateral import and therefore negligible external influence on P_{CO2}. Environmental factors such as T_{air} and water temperature (T_{water}), groundwater, and surface water are some examples of external influences which could obstruct a biological signal in P_{CO2}. Root respiration (R_{root}) and leaching of other root exudates could convert a fraction of CO_2 uptake by plants (GPP) into dissolved C in soil and water, which can then become part of lateral C flux. This is not unlike the plant-mediated relationship between GPP and subsequent methane flux (FCH_4) in wetlands (Gomez-Casanovas et al. 2020; Turner et al. 2021). Relating lateral and vertical fluxes is challenging due to the compounding effects of T_{air} and water level, which could interfere with potential correlations between GPP or R_{eco} and P_{CO2}. T_{air} will generally enhance wetland GPP but reduce P_{CO2}, while rising water level will typically increase GPP and P_{CO2} (Pugh et al. 2018).

Estimating Wetland Lateral Carbon Flows

Some evidence already exists for the relationship between lateral and vertical CO_2 flux in wetlands (Santos et al. 2019; Schneider et al. 2020; Bogard et al. 2020) and forests (Öquist et al. 2014). More specifically, previous studies have measured CO_2 concentrations and fluxes to understand their relative contributions to overall C balance at individual sites (Chu et al. 2015; Nilsson et al. 2008). This relationship needs to be further explored across different timescales because environmental controls that affect lateral and vertical fluxes could change from the daily to annual scale. Measuring the strength of correlation between lateral and vertical wetland CO_2 exchanges using GPP, R_{eco}, and dissolved CO_2 in wetland surface and porewater could improve our understanding of the link between fluxes and how they affect C sequestration and storage in water over time.

In this data synthesis, we expect differences between wetland types in terms of both hydraulic residence times (HRTs) and productivity. We hypothesize that the relationship between aquatic CO_2 concentration and ecosystem fluxes will differ across hydrologic wetland types (e.g., groundwater-fed fens, precipitation-fed bogs, tidal marshes, etc.) as a result. Average water travel time through an ecosystem or water body is represented as HRT (Kusin 2013) and has been measured in wetlands of various types (Arega et al. 2008; Etheridge et al. 2017; Sullivan et al. 2019; Winkler et al. 2016; Buytaert & Beven 2011; McJannet et al. 2012; Anderson & Lowry 2007; Maynard et al. 2009; Knox et al. 2008; Holloway 2010; Jordan et al. 2003; Gibson et al. 2000; Morris & Waddington 2011; Fleck et al. 2007; Gamble et al. 2003). Research shows tidal wetland HRT is typically shorter than other wetland types, followed by tidal creeks (Table 1). Fen wetland HRTs are greater and are inversely related to water level and discharge. Accordingly, HRTs in bogs are much longer than other wetland types due to their unique precipitation-dependent hydrology. Coupling between vertical and lateral CO_2 exchanges in wetland surface and porewater could disaggregate similarly to wetland types and HRTs, with stronger coupling in alpine wetlands and porewater due to longer HRTs, lower flow rate, and therefore less external influence on P_{CO2}. Comparing lateral and vertical fluxes across wetland types will expand our understanding of how GPP or R_{eco} relate to P_{CO2} and whether this conceptual framework is supported by observations.

How P_{CO2} Relates to Ecosystem Fluxes

Numerous processes factor into lateral and vertical exchange of wetland CO_2 (Fig. 1). Precipitation mixes with plant isoprene emissions, pollution, and dust to provide organic matter to soils below (Ward et al. 2017). Plant debris accumulates and decays initially at the soil surface. Photosynthetic uptake of atmospheric CO_2 and conversion into photosynthate supplies plant metabolism and the release of CO_2 through roots. Precipitation, root respiration of CO_2 and other exudates, and decaying plant material provide organic carbon (OC) for soil organisms to consume. Venting of CO_2

Table 1 Mean area-weighted average hydraulic residence times (HRTs) according to ecosystem type. Details about references used to make this table can be found in the Supplementary Information (Table S1)

Ecosystem	Marsh (excluding impounded marsh)	Tidal	Fen	Bog	Alpine	Porewater
Hydraulic residence time (HRT)	0.4 h	5.6 h	1.6 days	2.9 days	17.5 days	23.7 days

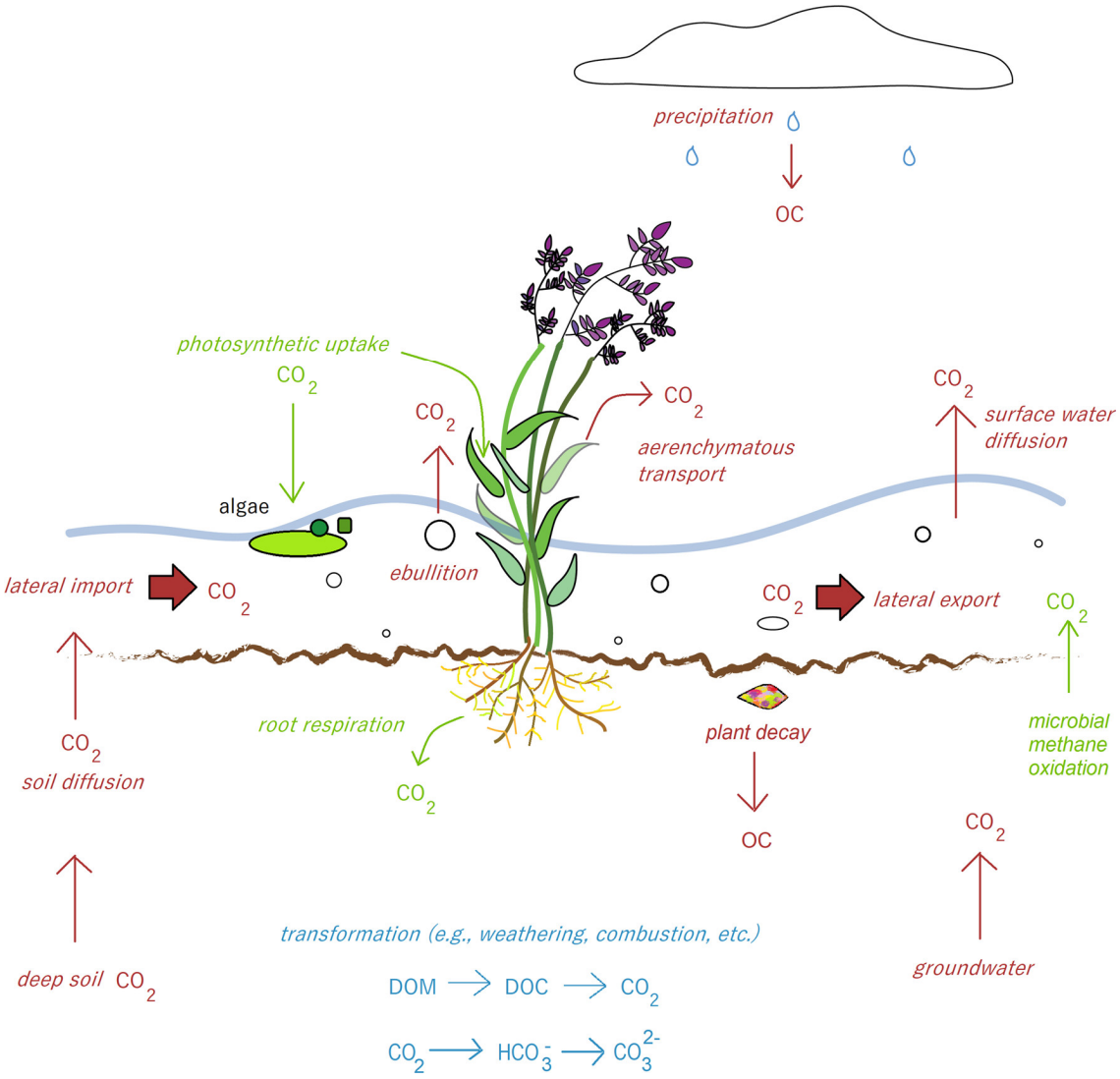

Fig. 1 Illustration of various contributions to lateral and vertical CO_2 wetland flux between soil, water, and air. Chemical processes (transformation) are in blue; physical processes (groundwater, plant decay, aerenchymatous transport, ebullition, precipitation, soil and surface water diffusion, lateral import and export) in red; biological processes (microbial methane oxidation, root respiration, photosynthesis) in green. DOM stands for dissolved organic matter, DOC stands for dissolved organic carbon, and OC represents organic carbon

through the shoots, transported by aerenchyma, can prevent toxic buildup of CO_2 and bicarbonate in plant roots (Kirk et al. 2019). Many of these processes are also conduits for the movement of wetland CH_4, such as aerenchyma, ebullition, groundwater infiltration, soil or surface water diffusion, and lateral import or export (Vroom et al. 2022; Villa et al. 2020). CH_4 produced in soils can also be transformed into CO_2 through oxidation by methanogens in saturated soils or the water column.

Groundwater is typically rich in CO_2 and its upwelling represents an important but highly spatially variable gas source to soil porewater, surface water, and eventually the atmosphere (Chen et al. 2023). Assessing the influence of groundwater on whole-ecosystem gas exchange is extremely challenging given its spatial and temporal variability. Global surface-water-to-groundwater turnover time at 25 m below surface is estimated to be ~ 10 years for aquatic ecosystems, which necessitates long-term monitoring studies to accurately estimate landscape-level carbon budgets and their decadal variability (Downing & Striegl 2018). Similarly, deep soil may release CO_2 to surface soils during the transition from warmer to colder months, which can then diffuse into surface and porewater (Campeau et al. 2021a). Lateral import of CO_2 tends to be lower than export in wetlands but is still a fundamental and understudied aspect of wetland C cycling.

Transformation of C is continuous as these dynamic wetland processes take place. Organic substrates and DOC are

biologically transformed (e.g., decomposition) into inorganic C. Labile DOC is oxidized to CO_2, which depending on water pH may form bicarbonate or carbonate, which is then exported laterally or released from surface water to the atmosphere. Additional processes contributing to the transformation and cycling of wetland C include weathering, snowfall, photo-oxidation, coastal outwelling, anthropogenic disturbances, bicarbonate buffering, and more. Transformation of wetland DOC into DIC is more thoroughly discussed from the coastal ecosystem perspective in Santos et al. (2021). Factors controlling temporal variability in tidal wetland DIC flux are discussed further in Wang et al. (2016b).

The primary objective of this study is to determine how GPP and R_{eco}, observed through the vertical flux of CO_2, relate to P_{CO2}, an important component of lateral flux, in wetlands. We do this by comparing GPP and R_{eco} to P_{CO2} concentrations at different timescales, measuring the strength of coupling, and determining whether it is a direct or indirect link. Analysis focused strongly on R_{eco}, rather than NEE, because it was expected to relate most closely with P_{CO2} due to root respiration. We hypothesize that GPP and R_{eco} are coupled to P_{CO2} in wetlands because of the physical connection between photosynthesizing plants, CO_2-respiring roots, and surface water and porewater. Furthermore, low lateral flow and higher HRTs should lead to a majority of on-site vertical exchange and respiration of P_{CO2}, which would become part of whole-ecosystem flux captured by the eddy covariance (EC) method. Low lateral flow should therefore lead to P_{CO2} being more directly connected to vertical flux components. Higher flow rates and lower HRTs should lead to the transportation and consumption of P_{CO2} outside of the flux tower footprint of an individual site, and a less pronounced relationship between P_{CO2} and GPP or R_{eco} due to EC measurements overlooking this portion of ecosystem gas exchange. A weaker link between P_{CO2} and vertical flux is also expected during times with higher lateral flow due to stronger input from other factors like groundwater, with different chemistry and age characteristics (Pint et al. 2003).

Methods

Experimental Design

Through an open call, we collected and synthesized measurements of lateral and vertical CO_2 flux across 22 Northern Hemisphere wetland sites (Fig. 2). Our goal was to collect data on GPP, R_{eco}, $P_{CO2,}$ and related variables (i.e., T_{air}, T_{water}, water table depth (WTD), discharge) across sub-diel, diel, and monthly scales to test the relationship between lateral and vertical wetland flux. To determine typical wetland soil porewater and surface water P_{CO2} concentrations (Question 1), we compared high-frequency P_{CO2} time series

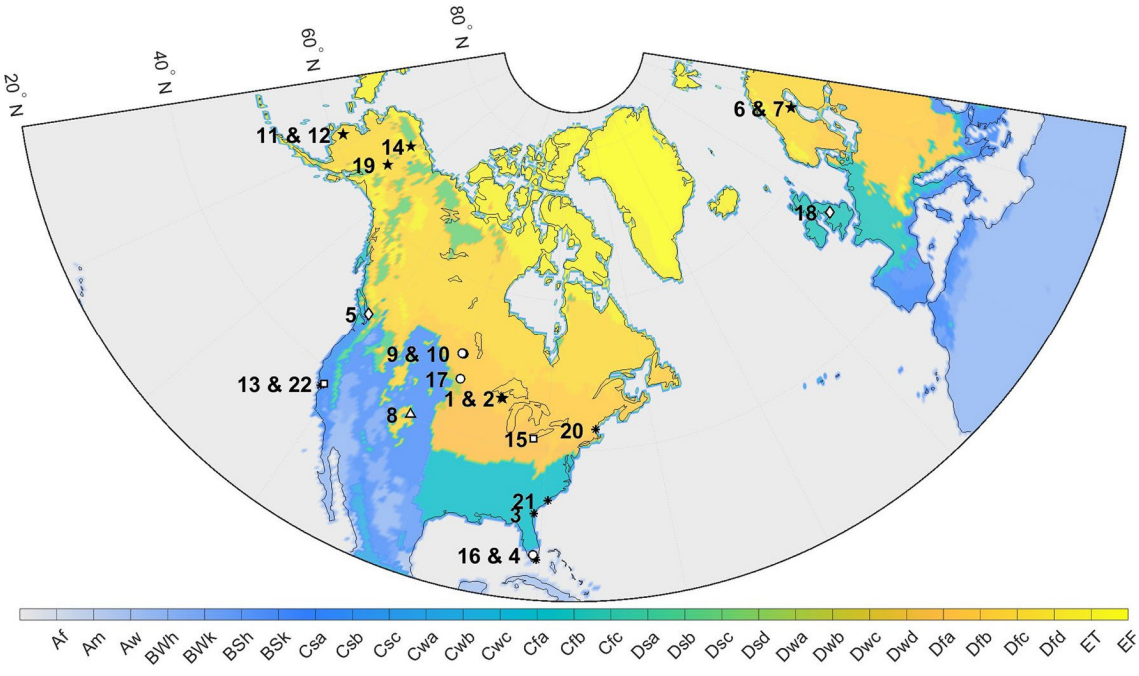

Fig. 2 Köppen climate map of study sites. Numbers represent each site listed in Table 2. Köppen classifications in the legend are listed according to the codes in Table S3 (Supplementary Information). Meridians are shown every 20° from -180 to 30°. Stars represent fens; asterisks indicate tidal systems; diamonds represent bogs; squares represent marshes; circles represent prairie potholes or karsts; and triangles symbolize alpine systems. The Koppen climate basemap was from Beck et al. (2018)

measurements from six different categories (alpine, marsh, tidal, fen, bog, and prairie pothole/karst) and multiple locations, and identified significant differences using ANOVA. There were 22 sites with sufficient surface water measurements and 9 with sufficient porewater measurements to answer this question.

To establish whether a relationship exists between lateral and vertical wetland CO_2 flux components (Question 2), we need data on P_{CO2}, GPP, and R_{eco} on a broad range of temporal scales. We tested our hypothesis that lateral and vertical wetland CO_2 flux components are related by comparing seasonal cycles of porewater and surface water P_{CO2} to R_{eco} and GPP at 3 sites with sufficient data (Eden Landing Ecological Reserve (US-EDN), Allequash Creek Wetland Site (US-ALQ), and Degerö Stormyr (SE-Deg)). Additionally, nonparametric regressions of lateral and vertical flux components were performed at sites with at least three months of concurrent half-hourly or hourly data. Five sites met this criterion (US-EDN, US-ALQ, US-Myb, US-Los, and SE-Deg).

The question of how discharge mediates the relationship between lateral and vertical flux components (Question 3) required concurrent sub-daily scale data on wetland R_{eco} or GPP, P_{CO2}, and discharge from multiple sites. To test our hypotheses, we identified a subset of three wetlands (US-EDN, US-ALQ, and SE-Deg) with sufficient data for further analysis. Lateral and vertical flux components from the subset were compared across times with low, medium low, medium, and high discharge rates at each site. These flow regimes were defined as 0-25th percentile, 25th-50th percentile, 50th-75th, and 75th-100th percentile discharge rates at each site.

Site Descriptions

Sites were found through web search (Google Scholar), solicited online (FLUXNET listserv, Twitter, email) and by word-of-mouth (Table 2). Sites included in the synthesis needed to have *in-situ* P_{CO2} data from within the wetland or in a nearby (< 1 km) wetland stream outlet, as well as light chamber flux measurements only for sites with dominant low-lying vegetation or EC flux measurements for sites with scrubs, shrubs, tall grasses, or tree cover. Observations of WTD and T_{air} or T_{water} were helpful but not necessary for sites to be included in analysis.

Tidal

Tidal wetlands featured in the study occupied both the east and west coasts of the United States (Fig. 2 and Table 2). Different fluctuations in tide height were observed during each tidal cycle across sites, with water level at some wetlands fully receding below the marsh surface every day and staying above the surface for the entire study duration at others. Further details on all wetlands included in the study can be found in the Supplementary Information.

Alpine

One alpine wetland located within the Loch Vale watershed of Rocky Mountain National Park, Colorado, was included in the study. The wetland is vegetated, but the surrounding watershed is dominated by bare rock. Snow cover can last up to 8 months of the year, making snowmelt and buildup of gases under snow and ice important means of gas production and transport.

Prairie Potholes and Karsts

Prairie potholes featured in the study included ecosystems of both Canadian and US Prairie Pothole Regions (PPR), which have been the subject of many studies on soil organic C stocks under different land management practices (Loder & Finkelstein 2020; Tangen & Bansal 2020; Bansal et al. 2021). These wetlands are shallow freshwater marshes formed by glaciers retreating from the landscape during the Pleistocene. Surface water is regulated mainly by precipitation and snowmelt, leading to bog-like hydrology. Sulfate-rich groundwater or sulfur-oxidizing microbes in the region also contribute to high rates of sulfate reduction and carbon mineralization, which ultimately increases ecosystem C storage (Dalcin Martins et al. 2017).

Seasonally flooded karst wetlands of the Big Cypress National Preserve in Florida have similar shallow depths, with bedrock interface occurring around 2 m or less (Ward et al. 2020). However, these depressional wetlands formed under much different conditions (e.g., carbonate bedrock dissolution) slightly more recently, during the transition from Pleistocene to Holocene. Groundwater lies on a shallow aquifer directly below the soil surface.

Bogs, Fens, and Marshes

Bogs featured in the study were previously disturbed for different reasons but have since been restored through active or passive rewetting techniques. Wetlands of the South Pennines, United Kingdom were dominated by sedge (*Eriophorum vaginatum* and *E. angustifolium*) whereas the Canadian peat bog was dominated by both sedge and moss (*Sphagnum* spp.).

Fens incorporated in the study had a range of freshwater sources, from upland forest runoff to river flow to mountain snowmelt. Fen wetlands had a range of disturbance levels, including preservation, natural burning, and draining followed by rewetting. Site locations included Alaska, the midwestern USA, and Sweden.

Table 2 Study sites used in analysis. Years do not necessarily represent continuous periods of measurement

Wetland type	Year(s)	Latitude, longitude	Köppen climate	Location	Site abbreviation	Reference	Site #
fen	2020	46.0827, -89.9792	Humid continental	Rhinelander, Wisconsin, USA	Lost Creek Wetland (US-Los)	Desai et al. 2022; Turner et al. 2019; Richardson et al. 2023d	1
fen	2021 (NEE & porewater P_{CO2}), 2014–2015 (stream P_{CO2})	46.0308, -89.6067	Humid continental	Rhinelander, Wisconsin, USA	Allequash Creek Site (US-ALQ)	Crawford et al. 2017; Olson 2023; Richardson et al. 2023c	2
tidal marsh	2021	31.4441, -81.2835	Humid subtropical	Sapelo Island, Georgia, USA	Georgia Coastal Ecosystems LTER (US-GCE)	Hawman et al. 2021; Turner et al. 2022; Turner 2022	3
tidal marsh	2022	25.3539, -80.3810	Savanna	Greater Everglades Ecosystem, Florida, USA	Everglades Saltwater Intrusion Marsh (US-EvM)	Yu et al. 2022; Malone et al. 2021; Zhao et al. 2021; Malone et al. 2014; Malone et al. 2013; Richardson 2023b	4
bog	2016–2017	49.1293, -122.9849	Mediterranean	Delta, British Columbia, Canada	Delta Burns Bog (CA-DBB)	D'Acunha et al. 2019; Christen & Knox 2022	5
fen	2015–2018 (surface water P_{CO2}), 2014–2017 (porewater P_{CO2})	64.1833, 19.5500	Subarctic	VästerbottenCounty, Sweden	Degerö Stormyr (SE-Deg)	Nilsson & Peichl 2020; Campeau et al. 2021b; Leach et al. 2016; Sagerfors et al. 2008	6
fen	2018–2022 (P_{CO2}), 2021–2022 (NEE)	64.181002, 19.837239	Subarctic	VästerbottenCounty, Sweden	Trollberget rewetted peatland site (Troll.)	Laudon et al. 2021	7
alpine fen	1996 (NEE), 2013–2019 (daily P_{CO2}), 2016–2017 (hourly P_{CO2})	40.2900, -105.6670	Subarctic	Rocky Mountain National Park, Colorado, USA	Loch Vale (LV)	Mast et al. 1998; Wickland et al. 2001; Clow et al. 2021a, b	8
prairie pothole	2021	50.3705, -100.5339	Humid continental	Manitoba, Canada	Manitoba Prairie Pothole Wetland, grassland (MBPPW1)		9
prairie pothole	2021	50.3623, -100.2024	Humid continental	Manitoba, Canada	Manitoba Prairie Pothole Wetland, cropland (MBPPW2)		10
fen & bog	2022	61.2723, -163.2228	Subarctic	Yukon Delta National Wildlife Refuge, Bethel, Alaska and St. Mary's Village, Alaska, USA	Yukon-Kuskokwim Delta, Izaviknek-Kingaglia uplands, Burned 2015 (YKD1)	Zolkos et al. 2022	11
fen & bog	2022	61.2548, -163.2590	Subarctic	Yukon Delta National Wildlife Refuge, Bethel, Alaska and St. Mary's Village, Alaska, USA	Yukon-Kuskokwim Delta, Izaviknek-Kingaglia uplands, Unburned (YKD2)	Zolkos et al. 2022	12
impounded marsh	2017–2021	38.0499, -121.7650	Mediterranean	Sherman Island, Sacramento County, California, USA	Mayberry wetland (US-Myb)	Hatala-Matthes et al. 2021; Detto et al. 2010	13

Table 2 (continued)

Wetland type	Year(s)	Latitude, longitude	Köppen climate	Location	Site abbreviation	Reference	Site #
fen	2007–2017	68.6058, -149.3110	Tundra	Imnavait Creek, Alaska, USA	Imnavait Creek Watershed Wet Sedge Tundra (US-ICs)	Kling 2019	14
freshwater marsh	2016	41.3795, -82.5125	Humid continental	Huron, Ohio, USA	Old Woman Creek (US-OWC)	Bohrer et al. 2019; Bohrer & Kerns 2022	15
karst	2015–2016 (P_{CO2} only)	25.9896, -80.9279	Savanna	Greater Everglades Ecosystem, Florida, USA	Big Cypress National Preserve (Big Cypress)	Ward et al. 2020	16
prairie pothole	2010–2016 (P_{CO2} only)	47.0992, -99.0992	Humid continental	Jamestown, North Dakota, USA	Cottonwood Lake Study Area (Cotton.)	Gleason et al. 2009; Tangen & Bansal 2017	17
bog	2022	53.5158, -1.9837	Temperate oceanic	South Pennines, UK	Restored peatlands of south Pennines (SP)		18
fen	2016	64.701, -148.313	Subarctic	Fairbanks, Alaska, USA	Alaska Peatland Experiment (APEX), includes US-BZF	Euskirchen 2022; Euskirchen et al. 2019; Euskirchen et al. 2017; Rupp 2019	19
tidal marsh	2018–2019	42.7345, -70.8382	Humid continental	Plum Island Sound, Massachusetts, USA	Plum Island Ecosystem (PIE), includes US-PHM and US-PLM	Giblin 2021; Feagin et al. 2020	20
tidal marsh	2020	33.3455, -79.1957	Humid subtropical	Georgetown, South Carolina, USA	North Inlet Crab Haul Creek (US-HB1)	Forsythe et al. 2020a; b	21
tidal marsh	2021	37.6156, -122.1140	Mediterranean	San Francisco Bay, California, USA	Eden Landing Ecological Reserve (US-EDN)	Shahan et al. 2022; Oikawa 2020	22

Surface water from only one freshwater marsh was included in the study. The wetland was impounded for restoration purposes, leading to low surface water flows between inlets and outlets controlled by wind and hydrologic management (Miller et al. 2008; Arias-Ortiz et al. 2021). Droughts in the region can lead to salinization due to evapoconcentration, saltwater intrusion, and reduction of typically constant water table levels.

Porewater

Sites with porewater data included two riverine fens, a boreal rich fen peatland, a range of wetland types (peatland plateaus, peatland ponds, and fen channels) in Alaska, and a flooded natural freshwater estuary with marsh hydrology. Dominant vegetation types varied across wetlands with porewater data. More details can be found in the Supplementary Information.

Data Processing

P_{CO2} was measured directly through automatic sampling at 8 sites, manual sampling at 11 sites, and both at 3 sites. P_{CO2} concentrations of manual samples were determined using gas chromatography with flame ionization detection (GC-FID) or isotope ratio mass spectrometry (IRMS). Automated sampling of P_{CO2} was performed with different infrared gas analyzers (IRGAs) across sites (Table S2). Eddy covariance CO_2 flux data (NEE) were gap-filled and partitioned into GPP and ecosystem respiration (R_{eco}) using marginal distribution sampling (MDS) and the daytime-based algorithm available through the online tool, REddyProc (Lasslop 2010; Wutzler et al. 2018). The micrometeorological convention used in this study is positive NEE for C source, negative NEE for C sink. Raw half-hourly flux data were made available upon request following site data sharing policies or collected through those available under the CC-BY4 license on FLUXNET or AmeriFlux archives. MATLAB scripts used for creating figures and calculating statistics provided in this manuscript are available online (Richardson 2023a). More details on sampling techniques, methods, and references can be found in Supplementary Information.

Statistical Testing

Significant differences in daily and annual average P_{CO2} concentrations according to wetland type were determined with ANOVA testing. Sites with at least 5 measurements for each hour, for at least 10 h per day, were included in diel cycle analysis (Figs S1-3). Although high frequency measurement was not a criterion for site selection, only sites with at least 5 months of data coverage from a single year were included in seasonal analysis (Figs S4&5), and monthly data were averaged together across years. Sites with at least three continuous months of daily-scale resolution or finer P_{CO2} were used to determine optimal measurement frequency (Fig S12). Sites with a T_{air} range of at least 10 °C were included in the comparison of T_{air} and P_{CO2} (Fig S13). Sites with a WTD range of 0.4 m or more were included in comparisons of WTD and P_{CO2} (Fig S14).

Coupling between P_{CO2} and vertical flux was evaluated based on the relationship between $\Delta P_{CO2\ at\ Tmean}$ in surface or porewater and R_{eco} or GPP. Significant, positive correlations between $\Delta P_{CO2\ at\ Tmean}$ and R_{eco} or GPP were interpreted as coupling. The influence of T_{water} was removed using Eq. 1 (Takahashi et al. 2002). T_{mean} is the average T_{water} in °C during the study period and T_{obs} is the observed T_{water}. T_{air} is used if there are no T_{water} data for the site. P_{CO2} at T_{mean} is the temperature normalized partial pressure of CO_2 (in µatm or ppmv). The sensitivity parameter, *b*, is a number between 0 and 0.05 calibrated at each site and the values calculated for the subsample sites are provided in the Supplementary Information (Table S5).

$$P_{CO2atTmean} = P_{CO2} e^{[b(T_{mean} - T_{obs})]} \quad (1)$$

$\Delta P_{CO2\ at\ Tmean}$ was estimated based on biologically derived P_{CO2} ($P_{CO2\ BIO}$) as the difference between the maximum and minimum daily average concentrations for each day (Eq. 2; Takahashi et al. 2002). Calibration was done by calculating the correlation coefficient between $P_{CO2\ at\ Tmean}$ and temperature after changing the sensitivity parameter by 0.001 and selecting the value that resulted in the lowest correlation coefficient, without becoming negative (i.e., overcorrecting for the influence of temperature).

$$\Delta P_{CO2atTmean} = (P_{CO2atTmean})_{max} - (P_{CO2atTmean})_{min} \quad (2)$$

Results

Patterns and Concentrations of P_{CO2} in the World's Key Wetland Types

Overall, there were more than 6,000 daily resolution P_{CO2} data points from wetland surface (74%) and porewater (26%), and 27 annual resolution P_{CO2} data points (81% surface, 19% porewater). Wetland type did not influence annual average P_{CO2} concentrations (ANOVA, $F_{df,df} = 1.55$, $p = 0.24$). However, seasonal P_{CO2} cycling did appear to be related to wetland type, and all wetlands included in the study demonstrated seasonal and diel cycles of P_{CO2}, GPP, and R_{eco} (Fig S1-6). Monthly average P_{CO2} typically reached the highest concentrations of the year sometime in August for most fens, bogs, marshes, prairie potholes and karsts, and porewater. The highest monthly average P_{CO2}

at these wetlands were observed at least one month after peak CO_2 uptake. The exception was the alpine wetland, where P_{CO2} peaked in April, prior to the month with the highest photosynthetic CO_2 uptake. Monthly average P_{CO2} at the alpine wetland appeared to be linked to snow depth (Fig S9). More concurrent alpine wetland data would be necessary to confirm this.

Surface water and porewater were supersaturated with CO_2 across all wetland types, as indicated by daily average concentrations above current atmospheric background of approximately 415 ppmv (Fig. 3). Diel P_{CO2} cycles varied across and within wetland types (Figs S1-3). For example, P_{CO2} followed a semidiurnal pattern (i.e., completing a full cycle twice a day) at only three of 4 tidal wetlands (Fig S7). The same wetlands with semidiurnal cycles in P_{CO2} also featured semidiurnal tidal cycles (Fig S8). P_{CO2} also appeared to fluctuate with T_{water} in some tidal wetlands (Fig S10) but was driven by changes in tide height in others (Fig S11). Daily average P_{CO2} was also dependent on wetland type (ANOVA $p < 1e\text{-}10$, $F_{df,df} = 181$). Daily average P_{CO2} was lowest at the alpine wetland at 811 ppmv on average and was statistically significantly different from the next highest categories of marshes (1,574 ppmv) and tidal wetlands (2,431 ppmv) (Fig. 3). Fens, bogs, and prairie potholes/karsts had similar daily average P_{CO2} concentrations, ranging from approximately 3,350 to 4,100 ppmv. Daily average porewater P_{CO2} was more than an order of magnitude higher than the highest daily average surface water concentrations at ~ 100,000 ppmv. The largest relative percent range of P_{CO2} within a single day was 1,872%, or more than 10 times the average concentration for that day and was observed at an impounded oligohaline marsh.

Relationship of P_{CO2} to Drivers

Monthly average photosynthetic CO_2 uptake reached a maximum in June for all wetland types. Fens and bogs demonstrated the lowest monthly average GPP compared to other wetland types. Annual mean GPP at the alpine wetland Loch Vale was on the higher end of published ranges for alpine tundra wetlands (118–631 gC m^{-2} yr^{-1}; Lu et al. 2017; Table S4). Cumulative annual GPP for the impounded marsh US-Myb was on the higher end of published ranges for coastal marshes (1,023–1513 gC m^{-2} yr^{-1}). Annual mean GPP for fens, bogs, and prairie potholes/karsts in this study aligned with published ranges for other peatlands (201–869 gC m^{-2} yr^{-1}) and freshwater shrub swamps (248–856 gC m^{-2} yr^{-1}). All wetland types demonstrated similar diel CO_2 fluxes, emitting less than 5 µmol m^{-2} s^{-1} CO_2 at night, and absorbing up to 14 µmol m^{-2} s^{-1} CO_2 during the day through photosynthesis from approximately 5 am until 8 pm, though this varies with latitude and time of year. The highest photosynthetic CO_2 uptake occurred towards the middle of the day for all sites, despite differences in diel cycles of P_{CO2}.

Wetland type influenced the relationship between P_{CO2} and T_{air}, as was evidenced by the strong correlation between P_{CO2} and T_{air} at the alpine wetland ($R = -0.96$, $p = 0$), which was higher than any other wetland site (Fig S13). T_{air} only had a significant negative impact on P_{CO2} at the alpine wetland. Fens, bogs, and marshes presented the highest significant positive correlations between daily average surface

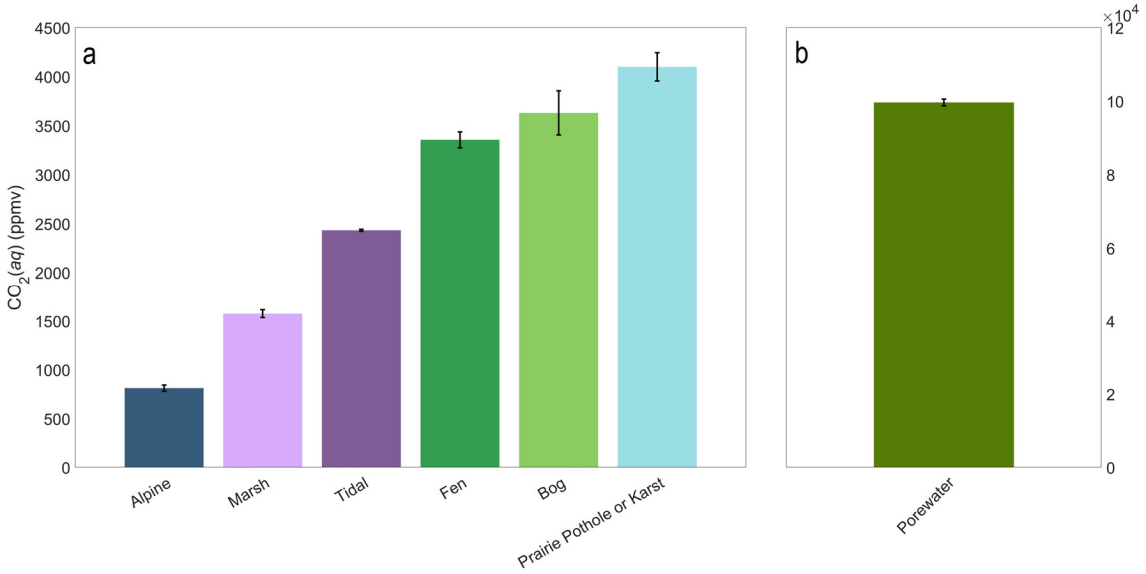

Fig. 3 Bar graph of daily average P_{CO2} in (**A**) surface water and (**B**) porewater across all wetland types. Error bars represent standard error of the mean

water P_{CO2} and T_{air} (R = 0.88 to 0.95, p < 0.05). Porewater P_{CO2} was also positively correlated to T_{air} across all sites with sufficient porewater data (R = 0.69 to 0.86, p < 0.05). The correlation between P_{CO2} and T_{air} was insignificant at prairie potholes/karsts and tidal wetlands (p > 0.05). The relationship between P_{CO2} and WTD was not as distinct. A positive correlation between P_{CO2} and WTD was only evident in surface water at two wetland sites; a marsh (R = 0.98, p < 0.001) and a prairie pothole (R = 0.99, p = 0.01). Results changed when comparing P_{CO2} and T_{water} instead of P_{CO2} and T_{air}, with impounded marsh US-Myb demonstrating a significant negative correlation (R = 0.74, p = 0.01), most likely driven by the reduction of CO_2 solubility with increasing T_{water}. Of the five sites with sufficient overlapping observations of P_{CO2} and T_{water}, there were positive correlations at only two sites, fen SE-Deg porewater (R = 0.97, p = 0.001) and fen US-ICs surface water (R = 0.88, p < <0.01). Correlations between P_{CO2} and T_{water} at the remaining sites were insignificant (Fig S14).

Seasonal changes of P_{CO2}, GPP, and R_{eco} were apparent in the three subsample sites, and monthly average GPP generally surpassed R_{eco} (Fig. 4). Daily resolution porewater P_{CO2} was significantly (p = 0) more strongly correlated with R_{eco} (R = 0.88) than GPP (R = 0.67) at US-ALQ. The same was true for SE-Deg porewater P_{CO2} and R_{eco} (R = 0.22) compared to SE-Deg porewater P_{CO2} and GPP (R = 0.12). Neither GPP nor R_{eco} were significantly (p > 0.05) correlated to surface water P_{CO2} at the tidal marsh. Correlation between GPP or R_{eco} and surface water P_{CO2} was similar in fens US-ALQ (R = 0.35, 0.34) and SE-Deg (R = 0.61, 0.68). Only fen SE-Deg exhibited significant correlations between NEE and P_{CO2}, though the relationship varied from weakly positive in porewater (R = 0.06, p = 0.03) to more negative in surface water (R = -0.39, p = 0.001).

Lateral and Vertical Fluxes are Not Linked by Discharge

A positive relationship between daily resolution R_{eco} and porewater $\Delta P_{CO2\ at\ Tmean}$ was observed at two out of 3 sites, and between R_{eco} and surface water $\Delta P_{CO2\ at\ Tmean}$ at two out of 3 sites. The strength of correlation varied across sites (Fig. 5). Although $\Delta P_{CO2\ at\ Tmean}$ in soil porewater at fen US-ALQ was positively correlated with R_{eco}, $\Delta P_{CO2\ at\ Tmean}$ in surface water at the same site was not. The largest observed difference between P_{CO2} and $\Delta P_{CO2\ at\ Tmean}$ averaged across the entire study period was in SE-Deg porewater, which was 1.157e5 ppmv. The smallest observed difference was in US-ALQ surface water, with a difference of 518 ppmv. A comparison of P_{CO2} and $\Delta P_{CO2\ at\ Tmean}$ for all subsample sites is provided in the supplementary information (Figure S17).

Random variations in daily scale correlation between lateral and vertical flux components appeared to be independent of fluctuations in discharge rate across sites (Fig. 6). Analysis of correlation coefficients between $P_{CO2\ at\ Tmean}$, GPP, and R_{eco} revealed that flow mediated the relationship between P_{CO2} and GPP at the tidal marsh (Fig S16), but not at either fen. Medium low flow corresponded with stronger coupling of P_{CO2} and GPP at the tidal marsh (R = -0.57, p = 0.005), though this could be a result of changing flow

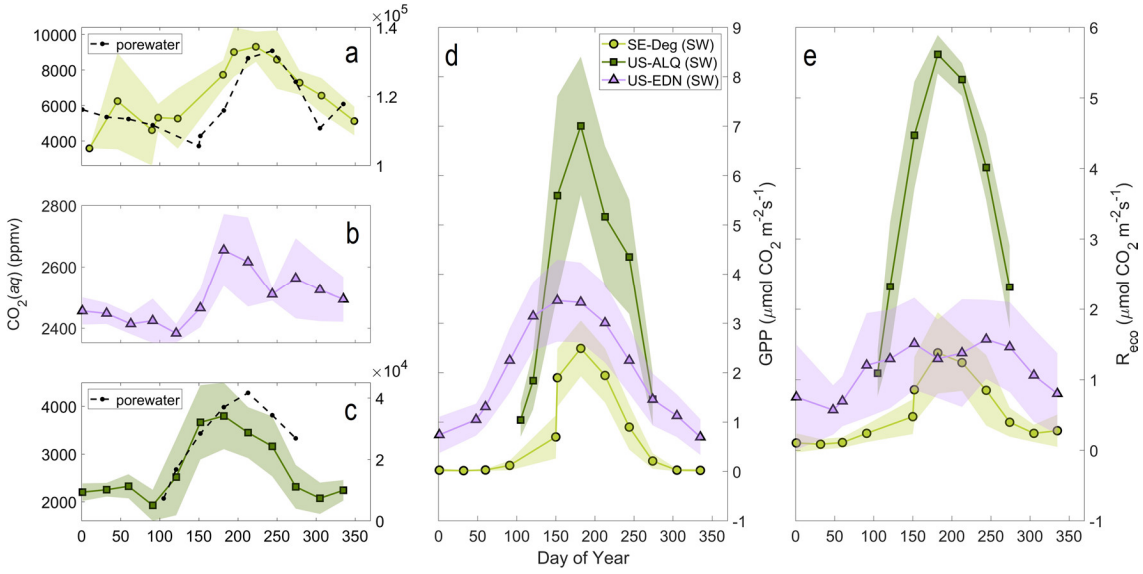

Fig. 4 Monthly averages of P_{CO2}: (**A**) in surface water (left axis) and soil porewater (right axis) at fen SE-Deg; (**B**) surface water at tidal marsh US-EDN; (**C**) surface water (left axis) and soil porewater (right axis) at fen US-ALQ; and monthly averages of (**D**) GPP (right axis) and (**E**) R_{eco} (right axis) at all three sites. Shaded areas display standard deviation

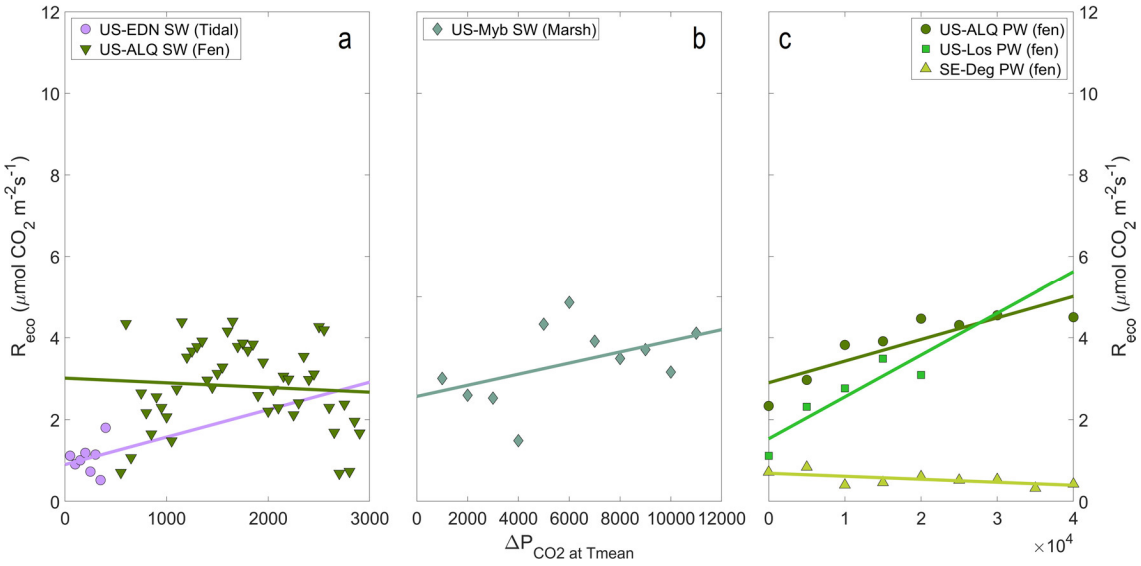

Fig. 5 Daily resolution $\Delta P_{CO2\ at\ Tmean}$ (ppmv) versus R_{eco} in (**A**) surface water, abbreviated SW, in a tidal wetland and fen bin-averaged every 50 ppmv, (**B**) nontidal marsh bin-averaged every 1,000 ppmv, and (**C**) porewater, abbreviated PW, bin-averaged every 5,000 ppmv. Solid lines represent the linear fit

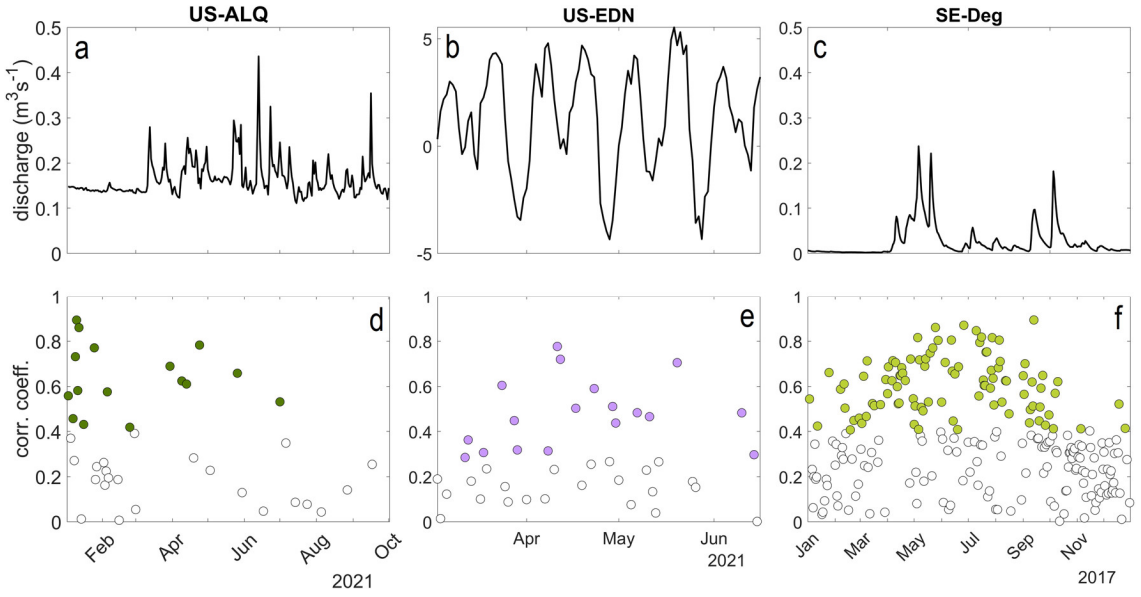

Fig. 6 Daily average discharge at (**A**) fen US-ALQ, (**B**) tidal marsh US-EDN, and (**C**) fen SE-Deg and corresponding correlation coefficients between half-hourly or hourly resolution $P_{CO2\ at\ Tmean}$ (see Eq. 1) and R_{eco} for each day in (**D**) US-ALQ surface water, (**E**) US-EDN surface water, and (**F**) SE-Deg porewater. Filled circles represent significant correlations. Only positive correlations are shown. Negative discharge suggests a change in the direction of surface water flow

direction (Fig S15). There were 11 low flow days at the tidal marsh with significant correlations between P_{CO2} and GPP ($R = 0.56$, $p << 0.01$), and 5 high-flow days with weaker, but significant correlations between P_{CO2} and GPP ($R = 0.36$, $p = 0.02$). The relationship between discharge and correlation coefficient between P_{CO2} and R_{eco} in the tidal marsh was insignificant ($p > 0.05$).

Results at the two subsample fens were similar, with similar correlation coefficients between sub-daily scale measurements of lateral and vertical flux components across flow regimes. Flow did not mediate the relationship between P_{CO2} and R_{eco} ($p > 0.05$), or GPP ($p > 0.05$) at fen SE-Deg. For example, there were 126 high-flow days with significant correlations between P_{CO2} and R_{eco} ($R = 0.67$, $p = 0.005$), and an

equally strong, significant correlation between P_{CO2} and R_{eco} on 100 days with medium low-flow ($R = 0.67$, $p = 0.006$) at the site. Correlation between P_{CO2} and R_{eco} was also independent of flow regime at US-ALQ ($p > 0.05$). There were four high-flow days with significant correlations ($R = 0.62$, $p = 0.008$) between hourly surface water P_{CO2} and R_{eco} and 8 medium low-flow days with equally strong, significant correlations ($R = 0.62$, $p = 0.007$) of P_{CO2} and R_{eco}. Only three low flow days demonstrated significant, positive correlation between P_{CO2} and GPP at fen US-ALQ ($R = 0.57$, $p = 0.01$). Seven medium low-flow days had significant correlations between P_{CO2} and GPP ($R = 0.52$, $p = 0.02$). There were no medium or high-flow days with significant P_{CO2} and GPP correlations at US-ALQ.

Discussion

Diel and Seasonal Cycles of Lateral and Vertical Wetland Flux Components

We hypothesized that R_{root} and root exudates would cause physical coupling between GPP or R_{eco} and P_{CO2}, with the strongest links occurring during times of low flow or in wetlands with longer HRTs and therefore lower flow rates. Results showed that GPP, R_{eco}, and P_{CO2} have similar seasonal cycles across all wetland types except alpine wetlands. P_{CO2} concentrations between wetland types are related on the daily scale but not at other timescales. Seasonal surface water P_{CO2} cycling bogs, fens, and freshwater marshes observed in this study were similar in magnitude to ranges provided by earlier studies of wetland ecosystems, but were higher than P_{CO2} concentrations in streams and ponds. For example, Johnson et al. (2010) found P_{CO2} in a peatland stream in Finland to range from approximately 610–2,036 ppm from April to June, which was similar in magnitude to the annual fluctuation in monthly average P_{CO2} in surface water at a marsh, fen, and alpine wetland presented in this study (US-Myb, US-ALQ, and LV; Fig S5).

Surface and porewater supersaturation across all wetland types matched expectations based on decomposition-limiting anerobic wetland conditions (Billett & Moore 2008; Aho & Raymond 2019). Although this would point to wetland surface and porewater as CO_2 sources from a thermodynamic standpoint, the combined effect of CO_2 uptake by photosynthetic organisms, coupled with the subsequent burial of organic matter, can surpass losses due to respiration or water–air evasion, which is lower in stagnant wetland surface waters than turbulently mixed water bodies (Koprivnjak et al. 2010).

Daily average P_{CO2} was more variable within and across wetland types than monthly averages (Figs S1, S5). Hydraulic residence times (HRTs) did appear to have a general impact on P_{CO2}, with daily average concentrations increasing from marshes to tidal wetlands, fens, and then bogs (Fig. 3). Wetland soil porewater across all wetland types also followed this rule, with higher HRT than surface water and much higher concentrations than wetland surface water. Alpine wetlands were an exception to this rule, possessing the largest HRTs but the lowest CO_2 concentrations compared to other wetland types. This could be due to HRT being lowest immediately following snowmelt in alpine ecosystems, then returning to a longer residence time for the rest of the unfrozen year. However, information on residence times at each site throughout the study period would be necessary to confirm this.

Diel fluctuation of wetland P_{CO2} observed at all sites in this study was similar to findings from other studies of aquatic ecosystems (Gómez-Gener et al. 2021; Rudberg et al. 2021; Attermeyer et al. 2021). In some rare instances, aquatic systems will lack any diel signal (Crawford et al. 2017). Diel P_{CO2} reached a maximum at nighttime in some wetlands, suggesting that root respiration increases P_{CO2} in surface water at night and strengthening our hypothesis that lateral and vertical CO_2 exchange are likely related. Diel P_{CO2} concentrations fluctuated by tens to thousands of ppmv from the highest to lowest point depending on the site and day (Fig S1). Manual sampling only at certain times of day, such as during low tide or daytime hours, could result in misrepresentation of daily average P_{CO2} concentration. Algal photosynthesis and DIC speciation due to bicarbonate buffering could also play a role in surface water CO_2 variability, but more information would be necessary to confirm this. Diel P_{CO2} fluctuation could also be due to higher midday water temperatures decreasing CO_2 solubility and releasing surface water CO_2 into the atmosphere. Other wetlands achieved maximum concentrations at midday, which was opposite to expectations if the two variables are linked (Fig S1). This relationship has previously been observed in an ultra-oligotrophic lake, where photosynthetic uptake was not clearly related to dissolved CO_2 (Eugster et al. 2022). Our analyses supported the idea that lateral and vertical CO_2 exchange in wetlands are not consistently strongly linked on the daily or seasonal scales.

Optimal Measurement Frequencies

Representativeness of local P_{CO2} sensor measurements at a broader spatial scale (e.g., flux tower footprint, entire wetland) is unknown. Additionally, transparent soil respiration chambers placed over vegetated zones will likely capture higher CO_2 fluxes as result of their influence on microbial respiration and other factors (Wang et al. 2016a). Annual average fluxes can also range between sinks and sources at different locations within the same forested site, as in Sakabe et al. (2015). As a result, we focused on seasonal and

diel cycles of P_{CO2} and GPP, averages across entire study periods, and direct links rather than P_{CO2} concentrations at individual sites or at specific times.

Optimal measurement frequency was determined to be the point at which the linear relationship between a subset of the original data had a correlation coefficient of R = 0.8 with the original dataset. There was a steep decline in representativeness of daily average P_{CO2} if half-hourly measurements were made less than once every 10 days, highlighting the usefulness of long-term measurement of P_{CO2} (Figure S10). Sub-daily scale measurements are also important for capturing the coherence between daily cycles of GPP and temperature-normalized P_{CO2} in some wetlands. Daily measurements should be made at least 50 times per year to accurately estimate annual average concentrations (R = 0.8 with annual means), and 3 or more times per month for accurate monthly average concentrations (R = 0.8 with monthly means).

Study Limitations

The main limitation of this study was the lack of data on the multiple external influences on wetland surface and soil porewater P_{CO2}, followed by a lack of wetland sites with concurrent high-frequency lateral and vertical CO_2 flux and concentration measurements. High-frequency, concurrent measurements of discharge rate and lateral import of P_{CO2} are essential to calculate net lateral export as P_{CO2}. Other information related to water residence times (e.g., flood depth and duration) could be valuable in explaining variations between lateral and vertical CO_2 flux and concentration. Groundwater, surface water, precipitation, and their carbonate chemistries all play varying roles in P_{CO2} concentrations and fluctuations across wetland types and are often site-specific.

Scientific understanding of wetland lateral CO_2 fluxes would also benefit from better spatial data resolution. There were no wetlands in our study from South America, which contains the largest wetland surface area out of any continent (Junk 2013). Concentrations of surface water P_{CO2} in floodplain wetlands of the northwestern Brazilian Amazon ranged 896–13,530 ppmv, the upper end of which is higher than the monthly average of most sites presented in this study (Belger et al. 2011). Streams and rivers of the central and southwestern Amazon Basin are similar, with P_{CO2} concentrations ranging approximately 890–13,250 ppm (Ellis et al. 2012). Forested wetlands near Lake Janauacá in the central Amazon basin of Brazil also had high P_{CO2}, ranging from 664–11,006 ppmv (Amaral et al. 2020). P_{CO2} in a sewage-fed aquaculture pond in the East Kolkata wetlands of India were even higher, reaching as high as 21,140 ppmv (Bhattacharyya et al. 2020). A study on wetland plant physiological performance under flooding stress in the Pantanal determined that the wetland plant communities are well adapted to changing soil conditions caused by intense flooding followed by an intense dry season (Dalmagro et al. 2016). Comparing seasonal and diel cycles of surface water and porewater P_{CO2}, R_{eco}, and GPP in tropical wetlands such as these will likely reveal unique and surprising relationships between environmental variables.

Directions for Future Research

Measuring and monitoring changes in P_{CO2} is valuable because it exchanges more readily with the atmosphere than other forms of DIC (which are non-gaseous). Tracking DIC speciation is also necessary for understanding short-term biological dynamics. Inorganic C is the least measured net ecosystem carbon balance (NECB) term and makes up the majority of hydrologic C export and the majority of soil C (Bogard et al. 2020; Maher et al. 2013; Leibowitz et al. 2018). Although wetland DOC export at some sites is estimated to be an order of magnitude lower than DIC export, its measurement is equally as important because it is often a limiting factor on biota and plays a role in microbial metabolism, nutrient cycling, UV light in the water column, and drinking water treatment (Megonigal & Neubauer 2009; Korbel & Hose 2011; Ritson et al. 2014).

Soil and porewater CO_2 concentrations in wetlands are disconnected from atmospheric fluxes (i.e., GPP, R_{eco}, NEE) because they are controlled by a multitude of other factors, which are deserving of further research. Such factors include anaerobic biological processes (e.g., methane oxidation) and physical processes (e.g., groundwater upwelling) which contribute to CO_2 buildup in wetland surface waters (Megonigal & Neubauer 2009). Air–water gas exchange can also be large and variable, giving rise over time to larger changes in the accumulation of aquatic CO_2 and its re-release into the atmosphere (Ward et al. 2017). The physics of wetland gas transport is an understudied avenue for further exploration.

Anaerobic mineralization of organic matter in wetland soils increases porewater pH and alkalinity, buffering coastal acidification (Sippo et al. 2016). Tidal wetlands with more marine exchange often feature higher soil inorganic C due to the higher settling and dissolution of $CaCO_3$, reducing P_{CO2} in the water column and increasing total alkalinity in the surrounding water (Mueller et al. 2023; Saderne et al. 2021). There are many opportunities for further exploration of the carbonate equilibrium and its impact on C storage in coastal systems. Areas that would benefit from further investigation are the quantification of total alkalinity export and calcium carbonate lateral flux between coastal ecosystems and the ocean, determining the fate of exported DIC as it moves downstream, the stability of the alkalinity buffer (i.e., how much DIC remains carbonate or bicarbonate versus how much is later evaded as CO_2?), and the proportion of total

alkalinity export due to carbonate sediment dissolution versus other sources (e.g., denitrification, fermentation, etc.).

New research is attempting to refine less understood aspects of the wetland C cycle by quantifying the coastal wetland contribution of DIC to the ocean or developing new frameworks for analyzing landscape-level fluxes. In fact, viewing wetland C within the context of watersheds as part of a net watershed exchange (NWE) could be the solution to improving estimations of lateral export (Casas-Ruiz et al. 2023). Our work suggests that as the planet warms and the contributions of different sources to runoff increase (e.g., rainfall) or decrease (e.g., snow and glacier melt), the influence on lateral export as P_{CO2} may be unpredictable (Cui et al. 2023). Long-term monitoring of discharge, GPP, R_{eco}, WTD, T_{air}, P_{CO2}, and HRTs could help improve our understanding of drivers of lateral CO_2 export from global wetlands.

Summary

This study was one of the first to evaluate water table, aquatic CO_2 concentration, and ecosystem gas exchange with eddy covariance across a range of wetland sites. Our study had the benefit of time series analysis over multiple years, rather than inferring relationships from discontinuous manual samples, which were the primary method of aquatic CO_2 sampling a generation ago. Linkages between lateral and vertical CO_2 exchange were examined according to wetland type by comparing seasonal and diel cycles, measuring the strength of coupling, and determining whether there was a direct or indirect link by removing the influence of T_{water} or T_{air} and estimating $\Delta P_{CO2\ at\ Tmean}$. Initially, it was believed that a possible relationship might exist between GPP, R_{eco}, and P_{CO2} due to the physical connection of photosynthesizing plants to surface and porewater through roots. We hypothesized that a signal from R_{root} would appear in dissolved CO_2 in wetlands with higher HRTs and during periods of low flow.

There were no statistically significant differences in yearly average P_{CO2} according to wetland type. However, daily average P_{CO2} was affected by wetland type, with alpine wetlands producing the lowest amounts of surface water dissolved CO_2, and the highest concentrations were in prairie potholes/karsts. Porewater P_{CO2} was at least an order of magnitude greater than the highest daily average surface water concentrations, likely due to heightened anoxia and the lack of wind-driven gas evasion below the soil surface. Air temperature was significantly negatively correlated with bin averaged P_{CO2} at an alpine wetland but had a positive correlation with P_{CO2} in other wetland sites, with the strongest relationships occurring in fens, bogs, and marshes. The connection between WTD and P_{CO2} was not consistent across or within wetland types. Periods of low discharge did not necessarily lead to higher correlations between GPP or R_{eco} and P_{CO2}.

Soil porewater and surface water ΔP_{CO2} were not consistently positively correlated with R_{eco} or GPP. Further study of wetland porewater and surface water P_{CO2} is essential to understand its complex relationships with other environmental variables and improve wetland C budgeting and ecosystem modeling. Our findings suggest that simple or direct universal relationships with eddy covariance flux tower estimates of GPP or R_{eco} and *in-situ* measurements of P_{CO2} to estimate or link lateral and vertical exchanges of CO_2 at wetlands are not likely to be found. Further research on wetland lateral CO_2 exchange could determine drivers of site-specific differences in P_{CO2} concentrations such as site-specific hydrology, aquatic chemistry (e.g., pH, salinity, etc.), spatial or interannual variability, and lag effects, and incorporate those relationships into ecosystem models. There remains a need for concurrent high resolution, long-term measurements of lateral and vertical greenhouse gas flux along with relevant ancillary data such as tide height or WTD and T_{air} or T_{water}. Higher quality data will help to remove the influence of external effects (e.g., weathering or tides) and allow studies to move past simple comparisons and correlations towards more advanced analytical methods to better identify environmental drivers of wetland gas emissions.

Supplementary Information The online version contains supplementary material available at https://doi.org/10.1007/s13157-023-01751-x.

Acknowledgements We would like to thank the scientists who helped us in the beginning stages of formulating our methods, especially Kenta Suzuki and Shin-ichiro S. Matsuzaki at the National Institute for Environmental Studies, and Nick Marzolf at Duke University.

Author Contributions Data collection, maintenance, and processing were performed by Jessica L. Richardson, Jonathan Thom, Kim Lindgren, Audrey Campeau, Dontrece Smith, Brenda D'Acunha, Darian Ng, Colin Edgar, Jason Dobkowski, Evan S. Kane, Gil Bohrer, Thomas O'Halloran, Jonny Ritson, Ariane Arias-Ortiz, Julie Shahan, and Maiyah Matsumura. Data interpretation and analysis was performed by Jessica L. Richardson, Ankur R. Desai, Hjalmar Laudon, Matthias Peichl, Mats Nilsson, Audrey Campeau, Järvi Järveoja, Peter Hawman, Deepak R. Mishra, Brenda D'Acunha, Sara H. Knox, Mark S. Johnson, Joshua Blackstock, Sparkle L. Malone, Steve F. Oberbauer, Matteo Detto, Kimberly P. Wickland, Inke Forbrich, Nathaniel Weston, Jacqueline K.Y. Hung, Eugenie S. Euskirchen, Syndonia Bret-Harte, George Kling, Evan S. Kane, Pascal Badiou, Matthew Bogard, Gil Bohrer, Thomas O'Halloran, Jonny Ritson, Ariane Arias-Ortiz, Dennis Baldocchi, Patty Oikawa, and Julie Shahan. The first draft of the manuscript was written by Jessica L. Richardson and all authors commented on previous versions of the manuscript. All authors read and approved the final manuscript.

Funding JR acknowledges support from the UW-Madison Student Research Grant Competition, PeatNeeds Microgrant from PeatECR Action Team, NSF, and the Eco-meteorology lab at UW-Madison. Funding for the AmeriFlux data portal is provided by the U.S.

Department of Energy Office of Science. US-EvM is supported in part by funds from the Department of Energy's National Institute for Climate Change Research grant (07-SC-NICCR-1059) and the National Science Foundation Division of Atmospheric & Geospace Sciences Atmospheric Chemistry Program awards (1561139, 1233006, and 1807533).

Data Availability Previously published data from sites in this manuscript can be accessed through the following citations: Desai 2023; Turner et al. 2019; Crawford et al. 2017; Olson 2023; Richardson et al. 2023c; Hawman et al. 2021; Turner et al. 2022; Turner 2022; Yu et al. 2022; Malone et al. 2021; Zhao et al. 2021; Malone et al. 2014; Malone et al. 2013; Richardson 2023b; D'Acunha et al. 2019; Christen & Knox 2022; Nilsson & Peichl 2020; Campeau et al. 2021b; Leach et al. 2016; Sagerfors et al. 2008; Laudon et al. 2021; Mast et al. 1998; Wickland et al. 2001; Clow et al. 2021a, b; Zolkos et al. 2022; Hatala-Matthes et al. 2021; Detto et al. 2010; Kling 2019; Bohrer et al. 2019; Bohrer & Kerns 2022; Ward et al. 2020; Gleason et al. 2009; Tangen & Bansal 2017; Euskirchen 2022; Euskirchen et al. 2019; Euskirchen et al. 2017; Rupp 2019; Giblin 2021; Feagin et al. 2020; Forsythe et al. 2020a, b; Shahan et al. 2022. These citations are also listed in Table S2. MATLAB scripts and daily average P_{CO2}, Reco, and GPP data for all sites are available in Richardson (2023a).

Declarations

Competing Interests The authors have no relevant financial or non-financial competing interests to disclose. Any mention of trade, firm, or product names is for descriptive purposes only and does not imply endorsement by the U.S. Government.

References

Aho KS, Raymond PA (2019) Differential response of greenhouse gas evasion to storms in forested and wetland streams. Journal of Geophysical Research: Biogeosciences 124:649–662. https://doi.org/10.1029/2018JG004750

Anderson MP, Lowry CS (2007) Transient functioning of a groundwater Wetland Complex, Allequash Basin, Wisconsin [PDF]. University of Wisconsin-Madison Water Resources Institute. https://digital.library.wisc.edu/1711.dl/ZPUTTIZBGZST38H

Arega F, Armstrong S, Badr AW (2008) Modeling of residence time in the East Scott Creek Estuary, South Carolina, USA. Journal of Hydro-Environment Research 2(2):99–108. https://doi.org/10.1016/j.jher.2008.07.003

Arias-Ortiz A, Oikawa PY, Carlin J, Masqué P, Shahan J, Kanneg S, ... Baldocchi DD (2021) Tidal and nontidal marsh restoration: A trade-off between carbon sequestration, methane emissions, and soil accretion. Journal of Geophysical Research: Biogeosciences 126(12):e2021JG006573. https://doi.org/10.1029/2021JG006573

Amaral JHF, Melack JM, Barbosa PM, MacIntyre S, Kasper D, Cortés A, ... Forsberg BR (2020) Carbon dioxide fluxes to the atmosphere from waters within flooded forests in the Amazon basin. Journal of Geophysical Research: Biogeosciences 125(3):e2019JG005293. https://doi.org/10.1029/2019JG005293

Attermeyer K, Casas-Ruiz JP, Fuss T, Pastor A, Cauvy-Fraunié S, Sheath D, ... Bodmer P (2021) Carbon dioxide fluxes increase from day to night across European streams. Communications Earth & Environment 2(1):1–8. https://doi.org/10.1038/s43247-021-00192-w

Bansal S, Tangen BA, Gleason RA, Badiou P, Creed IF (2021) Land management strategies influence soil organic carbon stocks of prairie Potholes of North America. Wetland Carbon and Environmental Management 273–285. https://doi.org/10.1002/9781119639305.ch14

Beck HE et al (2018) Present and future Köppen-Geiger climate classification maps at 1-km resolution. Scientific Data 5:180214. https://doi.org/10.1038/sdata.2018.214

Belger L, Forsberg BR, Melack JM (2011) Carbon dioxide and methane emissions from interfluvial wetlands in the upper Negro River basin, Brazil. Biogeochemistry 105(1):171–183. https://doi.org/10.1007/s10533-010-9536-0

Bhattacharyya S, Hazra S, Das S, Samanta S, Mukhopadhyay A, Dutta D, ... Chanda A (2020) Characterizing nutrient dynamics with relation to changes in partial pressure of CO2 in a tropical sewage-fed aquaculture pond situated in a Ramsar wetland. Water and Environment Journal 34(2):259–273. https://doi.org/10.1111/wej.12459

Billett MF, Moore TR (2008) Supersaturation and evasion of CO2 and CH4 in surface waters at Mer Bleue peatland, Canada. Hydrological Processes: An International Journal 22(12):2044–2054

Bogard MJ, Bergamaschi BA, Butman DE, Anderson F, Knox SH, Windham-Myers L (2020) Hydrologic export is a major component of coastal wetland carbon budgets. Global Biogeochemical Cycles 34(8):e2019GB006430. https://doi.org/10.1029/2019GB006430

Bohrer G, Ju Y, Arend K, Morin T, Rey-Sanchez C, Wrighton K, Villa J (2019) *Methane and CO2 chamber fluxes and porewater concentrations US-OWC Ameriflux wetland site, 2015–2018*. Environmental System Science Data Infrastructure for a Virtual Ecosystem (ESS-DIVE) (United States); AmeriFlux Management Project. https://doi.org/10.15485/1568865

Bohrer G, Kerns J (2022) AmeriFlux BASE US-OWC Old Woman Creek Ver. 3–5 AmeriFlux AMP. https://doi.org/10.17190/AMF/1418679

Buytaert W, Beven K (2011) Models as multiple working hypotheses: hydrological simulation of tropical alpine wetlands. Hydrological Processes 25(11):1784–1799. https://doi.org/10.1002/hyp.7936

Campeau A, Vachon D, Bishop K et al (2021) Autumn destabilization of deep porewater CO2 store in a northern peatland driven by turbulent diffusion. Nature Communications 12:6857. https://doi.org/10.1038/s41467-021-27059-0

Campeau A, Swedish University of Agriculture (2021b) Dataset for research article: Autumn destabilization of deep porewater CO2 store in a northern peatland driven by turbulent diffusion. Swedish national data service. Version 1. https://doi.org/10.5878/ggdt-ew12

Casas-Ruiz JP, Bodmer P, Bona KA, Butman D, Couturier M, Emilson EJ, Del Giorgio PA (2023) Integrating terrestrial and aquatic ecosystems to constrain estimates of land-atmosphere carbon exchange. Nature Communications 14(1):1571. https://doi.org/10.1038/s41467-023-37232-2

Chapin FS, Woodwell GM, Randerson JT, Rastetter EB, Lovett GM, Baldocchi DD, ... Schulze ED (2006) Reconciling carbon-cycle concepts, terminology, and methods. Ecosystems 9:1041–1050. https://doi.org/10.1007/s10021-005-0105-7

Chen K, Chen X, Stegen JC, Villa JA, Bohrer G, Song X, ... Zheng C (2023) Vertical hydrologic exchange flows control methane emissions from riverbed sediments. Environmental Science & Technology 57(9):4014–4026. https://doi.org/10.1021/acs.est.2c07676

Chu H, Gottgens JF, Chen J, Sun G, Desai AR, Ouyang Z, ... Czajkowski K (2015) Climatic variability, hydrologic anomaly, and methane emission can turn productive freshwater marshes into net carbon sources. Global Change Biology 21(3):1165–1181. https://doi.org/10.1111/gcb.12760

Ciais P, Borges AV, Abril G, Meybeck M, Folberth G, Hauglustaine D, Janssens IA (2008) The impact of lateral carbon fluxes on

the European carbon balance. Biogeosciences 5(5):1259–1271. https://doi.org/10.5194/bg-5-1259-2008

Clow DW, Qi SL, Akie GA (2021a) Continuous water-quality data for selected streams in Rocky Mountain National Park, Colorado, water years 2011–19: U.S. Geological Survey Data Release. https://doi.org/10.5066/P9RNS5FP

Clow DW, Striegl RG, Dornblaser MM (2021b) Spatiotemporal dynamics of CO2 gas exchange from headwater mountain streams. Journal of Geophysical Research: Biogeosciences 126(9):e2021JG006509. https://doi.org/10.1029/2021JG006509

Crawford JT, Stanley EH, Dornblaser MM, Striegl RG (2017) CO2 time series patterns in contrasting headwater streams of North America. Aquatic Sciences 79(3):473–486. https://doi.org/10.1007/s00027-016-0511-2

Christen A, & Knox S (2022) AmeriFlux FLUXNET-1F CA-DBB Delta Burns Bog. Lawrence Berkeley National Lab. (LBNL), Berkeley, CA (United States). AmeriFlux; University of British Columbia. https://doi.org/10.17190/AMF/1881565

Cui T, Li Y, Yang L, Nan Y, Li K, Tudaji M, ... Tian F (2023) Non-monotonic changes in Asian Water Towers' streamflow at increasing warming levels. Nature Communications 14(1):1176. https://doi.org/10.1038/s41467-023-36804-6

D'Acunha B, Morillas L, Black TA, Christen A, Johnson MS (2019) Net ecosystem carbon balance of a peat bog undergoing restoration: integrating CO2 and CH4 fluxes from eddy covariance and aquatic evasion with DOC drainage fluxes. Journal of Geophysical Research: Biogeosciences 124(4):884–901. https://doi.org/10.1029/2019JG005123

Dalcin Martins P, Hoyt DW, Bansal S, Mills CT, Tfaily M, Tangen BA, ... Wilkins MJ (2017) Abundant carbon substrates drive extremely high sulfate reduction rates and methane fluxes in Prairie Pothole Wetlands. Global Change Biology 23(8):3107–3120. https://doi.org/10.1111/gcb.13633

Dalmagro HJ, Lathuilliere MJ, Vourlitis GL, Campos RC, Pinto Jr OB, Johnson MS, ... Couto EG (2016) Physiological responses to extreme hydrological events in the Pantanal wetland: heterogeneity of a plant community containing super-dominant species. Journal of Vegetation Science 27(3):568–577. https://doi.org/10.1111/jvs.12379

Detto M, Baldocchi D, Katul GG (2010) Scaling properties of biologically active scalar concentration fluctuations in the atmospheric surface layer over a managed peatland. Boundary-Layer Meteorology 136:407–430. https://doi.org/10.1007/s10546-010-9514-z

Desai A (2023) AmeriFlux BASE US-Los Lost Creek, Ver. 26-5, AmeriFlux AMP, (Dataset). https://doi.org/10.17190/AMF/1246071

Desai AR, Murphy BA, Wiesner S, Thom JE, Butterworth BJ, Koupaei-Abyazani N, ... Davis KJ (2022) Drivers of decadal carbon fluxes across temperate ecosystems. Journal of Geophysical Research: Biogeosciences e2022JG007014. https://doi.org/10.1029/2022JG007014

Downing JA, Striegl RG (2018) Size, age, renewal, and discharge of groundwater carbon. Inland Waters 8(1):122–127. https://doi.org/10.1080/20442041.2017.1412918

Ellis EE, Richey JE, Aufdenkampe AK, Krusche AV, Quay PD, Salimon C, da Cunha HB (2012) Factors controlling water-column respiration in rivers of the central and southwestern Amazon Basin. Limnology and Oceanography 57(2):527–540. https://doi.org/10.4319/lo.2012.57.2.0527

Etheridge JR, Burchell MR II, Birgand F (2017) Can created tidal marshes reduce nitrate export to downstream estuaries? Ecological Engineering 105:314–324. https://doi.org/10.1016/j.ecoleng.2017.05.009

Eugster W, DelSontro T, Laundre JA, Dobkowski J, Shaver GR, Kling GW (2022) Effects of long-term climate trends on the methane and CO2 exchange processes of Toolik Lake, Alaska. Frontiers in Environmental Science 1457. https://doi.org/10.3389/fenvs.2022.948529

Euskirchen ES, Bret-Harte MS, Shaver GR, Edgar CW, Romanovsky VE (2017) Long-term release of carbon dioxide from arctic tundra ecosystems in Alaska. Ecosystems 20(5):960–974. https://doi.org/10.1007/s10021-016-0085-9

Euskirchen ES, Bret-Harte MS, Shaver GR, Edgar CW, Romanovsky VE (2019) Arctic Observatory Network: Imnavait fen eddy covariance. Arctic Observatory Network. http://aon.iab.uaf.edu/data_access. Accessed Oct 2023

Euskirchen E (2022) AmeriFlux BASE US-BZF Bonanza Creek Rich Fen Ver. 4–5 AmeriFlux AMP. https://doi.org/10.17190/AMF/1756433

Feagin RA, Forbrich I, Huff TP, Barr JG, Ruiz-Plancarte J, Fuentes JD, ... Miao G (2020) Tidal wetland gross primary production across the continental United States, 2000–2019. Global Biogeochemical Cycles 34(2):e2019GB006349. https://doi.org/10.1029/2019GB006349

Fleck JA, Fram MS, Fujii R (2007) Organic carbon and disinfection byproduct precursor loads from a constructed, non-tidal Wetland in California's Sacramento–San Joaquin Delta. San Francisco Estuary and Watershed Science 5(2). https://doi.org/10.15447/sfews.2007v5iss2art1 retrieved from https://escholarship.org/uc/item/4pb185j7. Accessed Oct 2023

Forsythe JD, Kline MA, O'Halloran TL (2020a) *AmeriFlux AmeriFlux US-HB1 North Inlet Crab Haul Creek*. Lawrence Berkeley National Lab. (LBNL), Berkeley, CA (United States). AmeriFlux; Clemson Univ, SC (United States). https://doi.org/10.17190/AMF/1660341

Forsythe JD, O'Halloran TL, Kline MA (2020b) An eddy covariance mesonet for measuring greenhouse gas fluxes in coastal South Carolina. Data 5(4):97. https://doi.org/10.3390/data5040097

Gamble JM, Burow KR, Wheeler GA, Hilditch R, Drexler JZ (2003) *Hydrogeologic data from a shallow flooding demonstration project, Twitchell Island, California, 1997–2001* (No. 2003–378). https://doi.org/10.3133/ofr03378

Giblin A (2021) AmeriFlux BASE US-PHM Plum Island High Marsh, Ver. 3–5, AmeriFlux AMP. https://doi.org/10.17190/AMF/1543377

Gibson JJ, Price JS, Aravena R, Fitzgerald DF, Maloney D (2000) Runoff generation in a hypermaritime bog–forest upland. Hydrological Processes 14(15):2711–2730. https://doi.org/10.1002/1099-1085(20001030)14:15%3c2711::AID-HYP88%3e3.0.CO;2-2

Gleason RA, Tangen BA, Browne BA, Euliss NH Jr (2009) Greenhouse gas flux from cropland and restored wetlands in the Prairie Pothole Region. Soil Biology and Biochemistry 41(12):2501–2507. https://doi.org/10.1016/j.soilbio.2009.09.008

Gomez-Casanovas N, DeLucia NJ, DeLucia EH, Blanc-Betes E, Boughton EH, Sparks J, Bernacchi CJ (2020) Seasonal controls of CO2 and CH4 dynamics in a temporarily flooded subtropical wetland. Journal of Geophysical Research: Biogeosciences 125(3):e2019JG005257. https://doi.org/10.1029/2019JG005257

Gómez-Gener L, Rocher-Ros G, Battin T, Cohen MJ, Dalmagro HJ, Dinsmore KJ, ... Sponseller RA (2021) Global carbon dioxide efflux from rivers enhanced by high nocturnal emissions. Nature Geoscience 14(5):289–294. https://doi.org/10.1038/s41561-021-00722-3

Hatala Matthes JA, Sturtevant C, Oikawa PY, Chamberlain SD, Szutu D, Arias-Ortiz A, ... Baldocchi D (2021) AmeriFlux BASE US-Myb Mayberry Wetland, Ver. 12–5, AmeriFlux AMP, *AmeriFlux AMP*. https://doi.org/10.17190/AMF/1246139

Hawman PA, Mishra DR, O'Connell JL, Cotten DL, Narron CR, Mao L (2021) Salt marsh light use efficiency is driven by environmental gradients and species-specific physiology and morphology. Journal of Geophysical Research: Biogeosciences 126(5):e2020JG006213. https://doi.org/10.1029/2020JG006213

Holloway RW (2010) Annual Sediment Retention and Hydraulic Residence Time Variability in a Riverine Wetland Receiving Unregulated Inflow from Agricultural Runoff. SNS Master's Theses. 28. https://digitalcommons.csumb.edu/sns_theses/28. Accessed Oct 2023

Johnson MS, Billett MF, Dinsmore KJ, Wallin M, Dyson KE, Jassal RS (2010) Direct and continuous measurement of dissolved carbon dioxide in freshwater aquatic systems—method and applications. Ecohydrology: Ecosystems, Land and Water Process Interactions, Ecohydrogeomorphology 3(1):68–78. https://doi.org/10.1002/eco.95

Jordan TE, Whigham DF, Hofmockel KH, Pittek MA (2003) Nutrient and sediment removal by a restored wetland receiving agricultural runoff. Journal of Environmental Quality 32(4):1534–1547. https://doi.org/10.2134/jeq2003.1534

Junk WJ (2013) Current state of knowledge regarding South America wetlands and their future under global climate change. Aquatic Sciences 75(1):113–131. https://doi.org/10.1007/s00027-012-0253-8

Kirk GJ, Boghi A, Affholder MC, Keyes SD, Heppell J, Roose T (2019) Soil carbon dioxide venting through rice roots. Plant, Cell & Environment 42(12):3197–3207. https://doi.org/10.1111/pce.13638

Kling G (2019) Biogeochemistry data set for Imnavait Creek Weir on the North Slope of Alaska 2002–2018. Arctic Data Center. https://pasta.lternet.edu/package/metadata/eml/knb-lter-arc/10531/8. Accessed Oct 2023

Knox AK, Dahlgren RA, Tate KW, Atwill ER (2008) Efficacy of natural wetlands to retain nutrient, sediment and microbial pollutants. Journal of Environmental Quality 37(5):1837–1846. https://doi.org/10.2134/jeq2007.0067

Koprivnjak J-F, Dillon PJ, Molot LA (2010) Importance of CO2 evasion from small boreal streams, Global Biogeochem. Cycles 24:GB4003. https://doi.org/10.1029/2009GB003723

Korbel KL, Hose GC (2011) A tiered framework for assessing groundwater ecosystem health. Hydrobiologia 661:329–349. https://doi.org/10.1007/s10750-010-0541-z

Kusin FM (2013) A review of the importance of hydraulic residence time on improved design of mine water treatment systems. World Applied Sciences Journal 26(10):1316–1322. https://doi.org/10.5829/idosi.wasj.2013.26.10.412

Lasslop G, Reichstein M, Papale D, Richardson AD, Arneth A, Barr A, Wohlfahrt G (2010) Separation of net ecosystem exchange into assimilation and respiration using a light response curve approach: Critical issues and global evaluation. Global Change Biology 16(1):187–208. https://doi.org/10.1111/j.1365-2486.2009.02041.x

Laudon H, Hasselquist EM, Peichl M, Lindgren K, Sponseller R, Lidman F, ... Ågren AM (2021) Northern landscapes in transition: Evidence, approach and ways forward using the Krycklan Catchment Study. Hydrological Processes 35(4):e14170. https://doi.org/10.1002/hyp.14170

Leach JA, Larsson A, Wallin MB, Nilsson MB, Laudon H (2016) Twelve year interannual and seasonal variability of stream carbon export from a boreal peatland catchment. Journal of Geophysical Research: Biogeosciences 121(7):1851–1866. https://doi.org/10.1002/2016JG003357

Leibowitz SG, Wigington PJ Jr, Schofield KA, Alexander LC, Vanderhoof MK, Golden HE (2018) Connectivity of streams and wetlands to downstream waters: An integrated systems framework. JAWRA Journal of the American Water Resources Association 54(2):298–322. https://doi.org/10.1111/1752-1688.12631

Loder AL, Finkelstein SA (2020) Carbon accumulation in freshwater marsh soils: A synthesis for temperate North America. Wetlands 40(5):1173–1187. https://doi.org/10.1007/s13157-019-01264-6

Lu W, Xiao J, Liu F, Zhang Y, Liu CA, Lin G (2017) Contrasting ecosystem CO 2 fluxes of inland and coastal wetlands: a meta-analysis of eddy covariance data. Global Change Biology 23(3):1180–1198. https://doi.org/10.1111/gcb.13424

Maher DT, Santos IR, Golsby-Smith L, Gleeson J, Eyre BD (2013) Groundwater-derived dissolved inorganic and organic carbon exports from a mangrove tidal creek: The missing mangrove carbon sink?, Limnology and Oceanography 58. https://doi.org/10.4319/lo.2013.58.2.0475

Malone SL, Zhao J, Kominoski JS, Starr G, Staudhammer CL, Olivas PC, ... Oberbauer SF (2021) Integrating aquatic metabolism and net ecosystem CO2 balance in short-and long-hydroperiod subtropical freshwater wetlands. Ecosystems 1–19. https://doi.org/10.1007/s10021-021-00672-2

Malone SL, Staudhammer CL, Oberbauer SF, Olivas P, Ryan MG, Schedlbauer JL, ... Starr G (2014) El Nino Southern Oscillation (ENSO) enhances CO2 exchange rates in freshwater marsh ecosystems in the Florida Everglades. PLoS One 9(12):e115058. https://doi.org/10.1371/journal.pone.0115058

Malone SL, Starr G, Staudhammer CL, Ryan MG (2013) Effects of simulated drought on the carbon balance of Everglades short-hydroperiod marsh. Global Change Biology 19(8):2511–2523. https://doi.org/10.1111/gcb.12211

Mast MA, Wickland KP, Striegl RT, Clow DW (1998) Winter fluxes of CO2 and CH4 from subalpine soils in Rocky Mountain National Park, Colorado. Global Biogeochemical Cycles 12(4):607–620. https://doi.org/10.1029/98GB02313

Maynard JJ, O'Geen AT, Dahlgren RA (2009) Bioavailability and fate of phosphorus in constructed wetlands receiving agricultural runoff in the San Joaquin Valley, California. Journal of Environmental Quality 38(1):360–372. https://doi.org/10.2134/jeq2008.0088

McJannet D, Wallace J, Keen R, Hawdon A, Kemei J (2012) The filtering capacity of a tropical riverine wetland: II. Sediment and nutrient balances. Hydrological Processes 26(1):53–72. https://doi.org/10.1002/hyp.8111

Megonigal JP, Neubauer SC (2009) Biogeochemistry of tidal freshwater wetlands. In: Perillo GME, Wolanski E, Brinson MM (eds) Coastal wetlands: An integrated ecosystem approach. Elsevier, Amsterdam, pp 535–562. https://doi.org/10.1016/B978-0-444-63893-9.00019-8

Mitra S, Wassmann R, Vlek PL (2005) An appraisal of global wetland area and its organic carbon stock. Current Science 88(1):25–35

Miller RL, Fram M, Fujii R, Wheeler G (2008) Subsidence Reversal in a Re-established Wetland in the Sacramento-San Joaquin Delta, California, USA. San Francisco Estuary and Watershed Science, 6(3). https://doi.org/10.15447/sfews.2008v6iss3art1. Retrieved from https://escholarship.org/uc/item/5j76502x

Morris PJ, Waddington JM (2011). Groundwater residence time distributions in peatlands: Implications for peat decomposition and accumulation. Water Resources Research 47(2). https://doi.org/10.1029/2010WR009492

Mueller P, Kutzbach L, Mozdzer TJ, Jespersen E, Barber DC, Eller F (2023) Minerogenic salt marshes can function as important inorganic carbon stores. Limnology and Oceanography 68(4):942–952

Nilsson, M. B., & Peichl, M. (2020). FLUXNET-CH4 SE-Deg Degero. FluxNet; Department of Forest Ecology and Management; Swedish University of Agricultural Sciences. https://doi.org/10.18140/FLX/1669659

Nilsson M, Sagerfors J, Buffam I, Laudon H, Eriksson T, Grelle A, ... Lindroth A (2008) Contemporary carbon accumulation in a boreal oligotrophic minerogenic mire–a significant sink after accounting for all C-fluxes. Global Change Biology 14(10):2317–2332

Oikawa P (2020) AmeriFlux BASE US-EDN Eden Landing Ecological Reserve, Ver. 2–5, AmeriFlux AMP. https://doi.org/10.17190/AMF/1543381

Olson, B. (2023). AmeriFlux FLUXNET-1F US-ALQ Allequash Creek Site. Lawrence Berkeley National Laboratory (LBNL), Berkeley, CA (United States). AmeriFlux; USGS. https://doi.org/10.17190/AMF/2006964

Öquist MG, Bishop K, Grelle A, Klemedtsson L, Kohler SJ, Laudon H, Nilsson MB (2014) The full annual carbon balance of boreal forests is highly sensitive to precipitation. Environmental Science & Technology Letters 1(7):315–319. https://doi.org/10.1021/ez500169j

Pint CD, Hunt RJ, Anderson MP (2003) Flowpath delineation and ground water age, Allequash Basin. Wisconsin Groundwater 41(7):895–902. https://doi.org/10.1111/j.1745-6584.2003.tb02432.x

Pugh CA, Reed DE, Desai AR, Sulman BN (2018) Wetland flux controls: how does interacting water table levels and temperature influence carbon dioxide and methane fluxes in northern Wisconsin? Biogeochemistry 137(1):15–25. https://doi.org/10.1007/s10533-017-0414-x

Richardson JL (2023a) turner-j/DissolvedCO2Synthesis: First Release (v1.0.0). Zenodo. https://doi.org/10.5281/zenodo.8102642

Richardson JL (2023b) Everglades saltwater intrusion marsh surface water dissolved CO2 June 19th to 25th 2022 ver 1. Environmental Data Initiative. https://doi.org/10.6073/pasta/94d3a758e245148df716e3c1c5fa7fed. (Accessed 2023-07-07)

Richardson JL, Desai AR, Thom J (2023c). Allequash creek wetland half-hourly soil porewater PCO2 2021 ver 1. Environmental Data Initiative. https://doi.org/10.6073/pasta/36bc6394ac59e09fcff390f316e96079. Accessed 7 Jul 2023

Richardson JL, Desai AR, Thom J (2023d) Lost Creek Wetland Soil Porewater PCO2 August to September 2020 ver 1. Environmental Data Initiative. https://doi.org/10.6073/pasta/70eaa7ee40dd318a216483f9499f3c49. Accessed 25 Sept 2023

Ritson JP, Graham NJD, Templeton MR, Clark JM, Gough R, Freeman C (2014) The impact of climate change on the treatability of dissolved organic matter (DOM) in upland water supplies: A UK perspective. Science of the Total Environment 473:714–730. https://doi.org/10.1016/j.scitotenv.2013.12.095

Rudberg D, Duc NT, Schenk J, Sieczko AK, Pajala G, Sawakuchi HO, Bastviken D (2021) Diel variability of CO2 emissions from northern lakes. Journal of Geophysical Research: Biogeosciences 126(10):e2021JG006246. https://doi.org/10.1029/2021JG006246

Rupp DL (2019) *Biogeochemical response to vegetation and hydrologic change in an Alaskan boreal fen ecosystem* (Doctoral dissertation, Michigan Technological University). https://doi.org/10.37099/mtu.dc.etdr/957

Saderne V, Fusi M, Thomson T, Dunne A, Mahmud F, Roth F, ... Duarte CM (2021) Total alkalinity production in a mangrove ecosystem reveals an overlooked Blue Carbon component. Limnology and Oceanography Letters 6(2):61–67

Sagerfors J, Lindroth A, Grelle A, Klemedtsson L, Weslien P, Nilsson M (2008) Annual CO2 exchange between a nutrient-poor, minerotrophic, boreal mire and the atmosphere. Journal of Geophysical Research 113:G01001. https://doi.org/10.1029/2006JG000306

Sakabe A, Kosugi Y, Takahashi K, Itoh M, Kanazawa A, Makita N, Ataka M (2015) One year of continuous measurements of soil CH4 and CO2 fluxes in a Japanese cypress forest: Temporal and spatial variations associated with Asian monsoon rainfall. Journal of Geophysical Research: Biogeosciences 120(4):585–599. https://doi.org/10.1002/2014JG002851

Santos IR, Maher DT, Larkin R, Webb JR, Sanders CJ (2019) Carbon outwelling and outgassing vs. burial in an estuarine tidal creek surrounded by mangrove and saltmarsh wetlands. Limnology and Oceanography 64(3):996–1013. https://doi.org/10.1002/lno.11090

Santos IR, Burdige DJ, Jennerjahn TC, Bouillon S, Cabral A, Serrano O et al (2021) The renaissance of Odum's outwelling hypothesis in "Blue Carbon" science. Estuarine, Coastal and Shelf Science 255:107361. https://doi.org/10.1016/j.ecss.2021.107361

Schneider CL, Herrera M, Raisle ML, Murray AR, Whitmore KM, Encalada AC, ... Riveros-Iregui DA (2020) Carbon dioxide (CO2) fluxes from terrestrial and aquatic environments in a high-altitude tropical catchment. Journal of Geophysical Research: Biogeosciences 125(8):e2020JG005844. https://doi.org/10.1029/2020JG005844

Shahan J, Chu H, Windham-Myers L, Matsumura M, Carlin J, Eichelmann E, ... Oikawa P (2022) Combining eddy covariance and chamber methods to better constrain CO2 and CH4 fluxes across a heterogeneous restored tidal wetland. Journal of Geophysical Research: Biogeosciences 127(9):e2022JG007112. https://doi.org/10.1029/2022JG007112

Sippo JZ, Maher DT, Tait DR, Holloway C, Santos IR (2016) Are mangroves drivers or buffers of coastal acidification? Insights from alkalinity and dissolved inorganic carbon export estimates across a latitudinal transect. Global Biogeochemical Cycles 30(5):753–766

Sullivan JC, Torres R, Garrett A (2019) Intertidal creeks and overmarsh circulation in a small salt marsh basin. Journal of Geophysical Research: Earth Surface 124:447–463. https://doi.org/10.1029/2018JF004861

Takahashi T, Sutherland SC, Sweeney C, Poisson A, Metzl N, Tilbrook B, ... Nojiri Y (2002) Global sea–air CO2 flux based on climatological surface ocean pCO2, and seasonal biological and temperature effects. Deep Sea Research Part II: Topical Studies in Oceanography 49(9–10):1601–1622. https://doi.org/10.1016/S0967-0645(02)00003-6

Tangen BA, Bansal S (2017) Soil properties and greenhouse gas fluxes of Prairie Pothole Region wetlands: a comprehensive data release. U.S. Geological Survey data release. https://doi.org/10.5066/F7KS6QG2

Tangen BA, Bansal S (2020) Soil organic carbon stocks and sequestration rates of inland, freshwater wetlands: Sources of variability and uncertainty. Science of the Total Environment 749:141444. https://doi.org/10.1016/j.scitotenv.2020.141444

Turner J, Desai AR, Thom J, Wickland KP, Olson B (2019) Wind sheltering impacts on land-atmosphere fluxes over fens. Frontiers in Environmental Science 179. https://doi.org/10.3389/fenvs.2019.00179

Turner J, Desai AR, Thom J, Wickland KP (2021) Lagged wetland CH4 flux response in a historically wet year. Journal of Geophysical Research: Biogeosciences 126(11):e2021JG006458. https://doi.org/10.1029/2021JG006458

Turner JL (2022) Sapelo Island Marsh pCO2, turbidity, and salinity, Summer 2021 ver 1. Environmental Data Initiative. https://doi.org/10.6073/pasta/972e85c197c3e30e27312ec6515ea2e9

Turner J, Desai AR, Blackstock J, Smith D (2022) Tidal influence on dissolved CO2 at Sapelo Island, Georgia, USA. Environmental Research: Ecology. https://doi.org/10.1088/2752-664X/aca0f4

Villa JA, Smith GJ, Ju Y, Renteria L, Angle JC, Arntzen E, ... Bohrer G (2020) Methane and nitrous oxide porewater concentrations and surface fluxes of a regulated river. Science of The Total Environment 715:136920. https://doi.org/10.1016/j.scitotenv.2020.136920

Vroom RJE, van den Berg M, Pangala SR, van der Scheer OE, Sorrell BK (2022) Physiological processes affecting methane transport by wetland vegetation-a review. Aquatic Botany 103547. https://doi.org/10.1016/j.aquabot.2022.103547

Wang H, Liao G, D'Souza M, Yu X, Yang J, Yang X, Zheng T (2016a) Temporal and spatial variations of greenhouse gas fluxes from a

tidal mangrove wetland in Southeast China. Environmental Science and Pollution Research 23(2):1873–1885. https://doi.org/10.1007/s11356-015-5440-4

Wang ZA, Kroeger KD, Ganju NK, Gonneea ME, Chu SN (2016b) Intertidal salt marshes as an important source of inorganic carbon to the coastal ocean. Limnology and Oceanography 61(5):1916–1931. https://doi.org/10.1002/lno.10347

Ward ND, Bianchi TS, Medeiros PM, Seidel M, Richey JE, Keil RG, Sawakuchi HO (2017) Where carbon goes when water flows: carbon cycling across the aquatic continuum. Frontiers in Marine Science 4:7. https://doi.org/10.3389/fmars.2017.00007

Ward ND, Bianchi TS, Martin JB, Quintero CJ, Sawakuchi HO, Cohen MJ (2020) Pathways for Methane Emissions and Oxidation that Influence the Net Carbon Balance of a Subtropical Cypress Swamp. Frontiers in Earth Science 8:573357. https://doi.org/10.3389/feart.2020.573357

Wickland KP, Striegl RG, Mast MA, Clow DW (2001) Carbon gas exchange at a southern Rocky Mountain wetland, 1996–1998. Global Biogeochemical Cycles 15(2):321–335. https://doi.org/10.1029/2000GB001325

Winkler G, Wagner T, Pauritsch M, Birk S, Kellerer-Pirklbauer A, Benischke R, ... Hergarten S (2016) Identification and assessment of groundwater flow and storage components of the relict Schöneben Rock Glacier, Niedere Tauern Range, Eastern Alps (Austria). Hydrogeology Journal 24(4):937. https://doi.org/10.1007/s10040-015-1348-9

Wutzler T, Lucas-Moffat A, Migliavacca M, Knauer J, Sickel K, Šigut L, Reichstein M (2018) Basic and extensible post-processing of eddy covariance flux data with REddyProc. Biogeosciences 15(16):5015–5030. https://doi.org/10.5194/bg-15-5015-2018

Yu Z, Staudhammer CL, Malone SL, Oberbauer SF, Zhao J, Cherry JA, Starr G (2022) Biophysical Factors Influence Methane Fluxes in Subtropical Freshwater Wetlands Using Eddy Covariance Methods. Ecosystems 1–18. https://doi.org/10.1007/s10021-022-00787-0

Zedler JB, Kercher S (2005) Wetland resources: status, trends, ecosystem services, and restorability. Annual Review of Environment and Resources 30:39–74. https://doi.org/10.1146/annurev.energy.30.050504.144248

Zhao J, Malone SL, Staudhammer CL, Starr G, Hartmann H, Oberbauer SF (2021) Freshwater wetland plants respond nonlinearly to inundation over a sustained period. American Journal of Botany 108(10):1917–1931. https://doi.org/10.1002/ajb2.1746

Zolkos S, MacDonald E, Hung JK, Schade JD, Ludwig S, Mann PJ, ... Natali S (2022) Physiographic controls and wildfire effects on aquatic biogeochemistry in Tundra of the Yukon-Kuskokwim Delta, Alaska. Journal of Geophysical Research: Biogeosciences 127(8):e2022JG006891. https://doi.org/10.1029/2022JG006891

Authors and Affiliations

Jessica L. Richardson[1] · Ankur R. Desai[2] · Jonathan Thom[3] · Kim Lindgren[4] · Hjalmar Laudon[5] · Matthias Peichl[5] · Mats Nilsson[5] · Audrey Campeau[5] · Järvi Järveoja[5] · Peter Hawman[6] · Deepak R. Mishra[6] · Dontrece Smith[7] · Brenda D'Acunha[8] · Sara H. Knox[9] · Darian Ng[9] · Mark S. Johnson[8] · Joshua Blackstock[10] · Sparkle L. Malone[11] · Steve F. Oberbauer[12] · Matteo Detto[13] · Kimberly P. Wickland[14] · Inke Forbrich[15] · Nathaniel Weston[16] · Jacqueline K. Y. Hung[17] · Colin Edgar[18] · Eugenie S. Euskirchen[18] · Syndonia Bret-Harte[18] · Jason Dobkowski[19] · George Kling[19] · Evan S. Kane[20] · Pascal Badiou[21] · Matthew Bogard[22] · Gil Bohrer[23] · Thomas O'Halloran[24] · Jonny Ritson[25] · Ariane Arias-Ortiz[26] · Dennis Baldocchi[26] · Patty Oikawa[27] · Julie Shahan[28] · Maiyah Matsumura[22]

✉ Jessica L. Richardson
Jturner5@lsu.edu

[1] Department of Oceanography & Coastal Sciences, Louisiana State University, Baton Rouge, LA, USA

[2] Department of Atmospheric & Oceanic Sciences, University of Wisconsin-Madison, Madison, MI, USA

[3] Space Science and Engineering Center, University of Wisconsin-Madison, Madison, MI, USA

[4] Unit for Field-Based Forest Research, Swedish University of Agricultural Sciences, Uppsala, Sweden

[5] Department of Forest Ecology & Management C, Swedish University of Agricultural Sciences, Uppsala, Sweden

[6] Department of Geography, University of Georgia, Athens, GA, USA

[7] Marine Institute, University of Georgia, Athens, GA, USA

[8] Department of Earth, Ocean, and Atmospheric Sciences, The University of British Columbia, Vancouver, Canada

[9] Department of Geography, The University of British Columbia, Vancouver, Canada

[10] USDA-ARS Dale Bumpers Small Farms Research Center, Booneville, AR, USA

[11] Yale School of the Environment, New Haven, CT, USA

[12] Institute of Environment and Department of Biological Sciences, Florida International University, Miami, FL, USA

[13] Department of Ecology and Evolutionary Biology, Princeton University, Princeton, NJ, USA

[14] U.S. Geological Survey, Geosciences and Environmental Change Science Center, Denver, CO, USA

[15] Marine Biological Laboratory, Woods Hole, MA, USA

[16] Department of Geography and the Environment, Villanova University, Villanova, PA, USA

[17] Woodwell Climate Research Center, Woods Hole, MA, USA

[18] Institute of Arctic Biology, University of Alaska Fairbanks, Fairbanks, AK, USA

[19] Department of Ecology & Evolutionary Biology, University of Michigan Ann Arbor, Ann Arbor, MI, USA

[20] College of Forest Resources and Environmental Science, Michigan Technological University, Houghton, MI, USA

[21] Ducks Unlimited Canada, Institute for Wetland and Waterfowl Research, Stonewall, Canada

[22] Department of Biological Sciences, University of Lethbridge, Lethbridge, AB, Canada

[23] Civil, Environmental and Geodetic Engineering, The Ohio State University, Columbus, OH, USA

[24] Clemson University, Clemson, SC, USA

[25] The University of Manchester, Manchester, UK

[26] Department of Environmental Science Policy and Management, University of California, Berkeley, CA, USA

[27] Earth and Environmental Sciences Department, CSU East Bay, Hayward, CA, USA

[28] Earth System Science, Stanford University, Stanford, CA, USA